THE ASTROPHYSICAL JOURNAL, 401:288–310, 1992 December 10

AN INTERPRETATION OF THE SPECTRAL PROPERTIES OF HOT HYDROGEN-RICH WHITE DWARFS WITH STRATIFIED H/He MODEL ATMOSPHERES

STÉPHANE VENNES[1]
Department of Physics and Astronomy, University of Delaware, Newark, DE 19716
AND
GILLES FONTAINE
Département de Physique, Université de Montréal, C.P. 6128, Montréal, Quebec, Canada H3C 3J7
Received 1992 March 27; accepted 1992 June 18

ABSTRACT

We present a grid of stratified H/He model atmospheres which are of particular interest for analyzing the EUV/soft X-ray observations of hot DA white dwarfs, and also for interpreting the optical spectra of DAO and DAB stars. The grid covers the range of effective temperature 25,000 K $\leq T_{\rm eff} \leq$ 65,000 K and the range of hydrogen layer mass $-17 \leq \log q_{\rm H} = \log (M_{\rm H}/M_{*}) \leq -13$. The adopted gravity is $\log g = 8$. The abundance profile in the H/He compositional transition zone is described in terms of pure diffusive equilibrium between gravitational settling and ordinary diffusion. We discuss the characteristic features of these models, including synthetic spectra covering the soft X-ray to the far-ultraviolet (FUV) as well as the optical domain for representative cases. With the help of these models, we next reanalyze critically the samples of hot DA white dwarfs which have been observed with *EXOSAT* and *Einstein*. Using conservative selection criteria, we find that six objects out of six with $T_{\rm eff} \leq$ 35,000 K do not show a EUV/soft X-ray flux deficiency and, therefore, can be understood solely in terms of pure hydrogen atmospheres. In contrast, a majority (six objects out of eight) of DA white dwarfs hotter than this value do show a flux deficiency and therefore require the presence of some absorbers in their atmospheres (currently believed to be provided by either the helium diffusive tail in a stratified atmosphere or by a complex of heavy elements levitating at low abundances in the radiation field). We show that the *EXOSAT* broad-band photometry of Feige 24 and G191 B2B cannot be explained in terms of stratified atmospheres. Absorption by heavy elements is most certainly responsible for the required EUV/soft X-ray opacity source in these cases. However, the *EXOSAT* data are consistent with the hypothesis of stratified atmospheres in the four remaining objects: GD 2, GD 153, GD 246, and GD 394. The inferred hydrogen layer masses for these stars are in the range $q_{\rm H} \approx 10^{-13.9}$–$10^{-13.5}$. We cannot totally rule out absorption by heavy elements in the atmospheres of these four objects at this stage, however, and we suggest that EUV *spectroscopy* be carried out on them since atmospheric stratification and absorption by heavy elements leave quite distinct signatures in the EUV spectral range. Finally, we briefly discuss the cases of the optical spectra of DAO and DAB stars in terms of our stratified model atmospheres.

Subject headings: diffusion — stars: abundances — stars: atmospheres — ultraviolet: stars — white dwarfs

1. INTRODUCTION

Observations of hot DA white dwarfs in the EUV/soft X-ray range have revealed that, in many cases, the detected flux is less than expected from pure hydrogen atmospheres. This implies an extra opacity source which must be due to the presence of small traces of heavier elements. With current available data, these elements are generally not spectroscopically detected in hot DA white dwarfs, but the large sensitivity of the EUV/soft X-ray broad-band flux to the presence of extra absorbers can be used to *infer* their abundances. For simplicity, it has been assumed that only helium provides the required opacity source in the majority of the analyses carried out so far. In addition, it has generally been assumed that helium is *uniformly* distributed in the atmosphere of a DA white dwarf. Thus, the presence of small uniform traces of helium has been invoked to explain the EUV/soft X-ray flux deficiency discovered in a large fraction of hot DA stars observed with *Einstein* (Kahn et al. 1984; Petre, Shipman, & Canizares 1986) and *EXOSAT* (Jordan et al. 1987; Paerels & Heise 1989). The potential presence of helium in earlier investigations was also suggested in the cases of Feige 24 (*Apollo-Soyuz*: Margon et al. 1976) HZ 43 (*Apollo-Soyuz*: Auer & Shipman 1977 and Heise & Huizenga 1980; suborbital rocket: Malina, Bowyer, & Basri 1982), and Sirius B (*Apollo-Soyuz*: Shipman et al. 1977).

Vennes et al. (1988) have recently reviewed in details the mechanisms that could be responsible for the presence of small traces of helium in the atmospheres of hot DA white dwarfs. They have favored a model in which these stars are interpreted as stratified objects with an outer layer of hydrogen which is sufficiently thick that radiation in the visible excapes only from H-rich regions, and yet sufficiently thin that the EUV/soft X-ray radiation escapes from deeper layers, polluted by the tail of the helium distribution which extends upwards. In this model, the bulk of the EUV/soft X-ray observations can be accounted for if, as a class, hot DA white dwarfs have very thin outer layers with estimated masses in the range $-13 \leq \log q_{\rm H} \leq -15$.

An alternative explanation to stratified atmospheres is the possibility that a host of heavy elements, including small traces of He, are present in the H-dominated atmospheres of hot DA white dwarfs with abundances below most current spectroscopic detectability limits. This possibility has been briefly

[1] Postal address: University of California at Berkeley, Center for EUV Astrophysics, 2150 Kittredge Street, Berkeley, CA 94720.

alluded to by Vennes et al. (1988) and has been recognized earlier by many other investigators. In this context, Vennes et al. (1989a) have convincingly demonstrated that the *EXOSAT* EUV spectrum of the hot DA white dwarf Feige 24 is incompatible with the idea of a H/He layered atmosphere, but can be nicely accounted for by absorption caused by a complex of heavy elements supported at low abundances by radiative levitation. Unfortunately, this is the only case where a definitive test between the two distinct possibilities could be carried out; the appropriate data (i.e., EUV spectra) are not currently available for other stars which require an extra EUV/soft X-ray opacity source. Note, however that Feige 24 is one of only a handful of hot DA stars which exhibit narrow photospheric heavy element lines in its ultraviolet spectrum (Dupree & Raymond 1982). A critical search of *IUE* high-dispersion spectra for DA stars observed also with *EXOSAT* has led Vennes, Thejll, & Shipman (1991a, hereafter VTS) to suggest that in some cases (such as Feige 24) heavy elements provide the required EUV/soft X-ray opacity. In other cases, where heavy element lines are not detected and only upper limits on abundances are available from *IUE* spectroscopy, the alternative possibility appears to be a H/He stratified atmosphere.

Irrespective of the situation in the short-wavelengths range of the spectrum, the case for layered atmospheres remains compelling for the DAO stars which are the hot progenitors of (at least some of) the ordinary DA stars. DAO stars display optical He I/He II and ultraviolet He II lines as well as the H I Lyman and Balmer lines (Wesemael, Green, & Liebert 1985; Holberg et al. 1989). Vennes et al. (1988) have shown that a stratified configuration is the only viable model for these stars. As evolution proceeds, they cool to become ordinary DA white dwarfs and, presumably, retain their layered configuration. Stratified atmospheres are also of great interest for interpreting the spectra of peculiar objects such as GD 323, the prototype of the DAB class of white dwarfs (Liebert et al. 1984). For instance, Koester (1989a) has suggested a stratified model with $T_{\rm eff} \approx 27{,}000$ K and a very thin outer hydrogen layer, $\log q_{\rm H} \approx -16.9$, to account for the simultaneous presence of H I and He I lines in the optical spectrum of GD 323.

Historically, the stratified atmospheric configuration was first proposed by Heise & Huizenga (1980) for their study of HZ 43, and also by Muchmore (1982) in a more general context. These pioneering studies suffered from their common assumption that the chemical composition changes discontinuously (from He-rich to H-rich) at some selected location in the atmosphere. Nevertheless, the synthetic spectra of Heise & Huizenga (1980) do display the essential spectral characteristic of stratified model atmospheres, namely the rapid flux fall-off shortward of the He II, $n = 1$ bound-free edge (see § 3). Their comparison between H/He homogeneous and stratified models allows to identify correctly their distinctive qualitative properties. An important improvement was introduced by Jordan & Koester (1986) by considering the condition of diffusive equilibrium in the computation of a realistic composition profile. The compositional transition zone between the H-rich and the He-rich layers in a typical hot DA atmosphere covers several pressure scale heights and is, therefore, of fundamental importance in the computation of the atmospheric structure. Jordan & Koester (1986) were interested in the unusual optical spectrum of GD 323 and computed models with rather thin hydrogen layers. Similar models but extending to larger hydrogen layer masses were subsequently presented by Koester (1989a, b) and Koester et al. (1990) in their analyses of *EXOSAT* observations of hot DA stars. More recently, Unglaub & Bues (1991) have initiated a model atmosphere program including carbon in a H/He/C stratified scheme. This approach may eventually find an application in the hot PG 1159−035 stars, which according to Werner, Heber, & Hunger (1991) have their atmospheres dominated by helium and carbon.

Our own interest in stratified model atmospheres derives from the work of Vennes et al. (1988) who were the first to make the case for thin hydrogen layers in hot DA white dwarfs as a possible general explanation for the EUV/soft X-ray flux deficiency observed in many objects. Except for ordinary diffusion (driven by a concentration gradient), there is no known physical mechanism potent enough to defeat gravitational settling of helium in the high-gravity, radiative atmospheres of hot DA white dwarfs to the point of maintaining abundances of helium sufficiently large to account for the required EUV/soft X-ray opacity. Only when the amount of hydrogen is of the order of the mass of the photospheric layers does ordinary diffusion compete efficiently against gravitational settling in the atmosphere, however. In that case, the state of diffusive equilibrium between the two processes is very rapidly reached. This leads to a highly *nonuniform* distribution of helium in the atmospheric layers, in conflict with the idea of *uniform* traces for helium postulated in most previous analyses of the EUV/soft X-ray observations of hot DA white dwarfs. Interestingly, using column density arguments, Vennes et al. (1988) were able to show that, at a given wavelength, there is a one-to-one correspondence between the helium abundances inferred on the basis of uniformly mixed H/He models and the hydrogen layer masses of stratified models in diffusive equilibrium. This useful demonstration has allowed the use of the previous analyses based on the assumption of uniform traces of helium in DA white dwarfs (Vennes et al. 1988). However, for improved analyses of individual objects, taking into account the details of the instrumental response of various detectors and bandpasses convolved with the wavelength-dependent effect of ISM opacity, it became clear that full model atmosphere calculations including the complication of vertical stratification in composition needed to be tackled.

To follow up on our previous work, we have consequently carried out the computation of a grid of stratified H/He model atmospheres applicable to the interpretation of the spectral properties of hot ($T_{\rm eff} \geq 25{,}000$ K) H-rich white dwarfs. The first goal of the present paper is to describe these models and their salient features. More details can be found in Vennes (1988). The models are fully characterized using synthetic spectra of the optical, the ultraviolet (covered by *IUE* and the *Hubble Space Telescope*) and the EUV/soft X-ray domains (explored mainly by *EXOSAT* and *Einstein*, currently covered by *ROSAT*, and soon to be studied spectroscopically with *EUVE*). The model atmospheres are described in § 2, and the emergent energy distributions from the models are presented in § 3. A preliminary report of these models has been presented by Vennes, Fontaine, & Wesemael (1989b), and an application to two hot DA white dwarfs was discussed in Vennes, Shipman, & Petre (1990).

In the second part of this paper (§ 4), we interpret the relevant observational data currently available for hot H-rich white dwarfs in terms of our stratified model atmospheres. We concentrate primarily on the samples of hot DA white dwarfs observed with *EXOSAT* and *Einstein*, but we also discuss briefly the cases of DAO and DAB stars. For DA objects observed in the EUV/soft X-ray spectral range, our approach

implicitly assumes that helium *alone* provides the required extra opacity (when needed). This ignores the very real possibility that absorption by heavy elements (as alluded to above) may play a significant role in some or even many of these stars. It is also known (see, e.g., Vennes et al. 1990) that the reality of the EUV/soft X-ray flux deficiency in hot DA stars is critically dependent on the accuracy with which the effective temperature is determined. We have therefore made an effort to provide improved determinations of the atmospheric parameters of these stars with previous uncertain parameters. In this effort, following the method of Vennes et al. (1990), we have made extensive use of *IUE* archived data on ultraviolet energy distributions as well as published optical photometry. We discuss the results of our investigations in § 5.

2. COMPUTATION OF A GRID OF H/HE STRATIFIED MODEL ATMOSPHERES

The model atmospheres are in local thermodynamic equilibrium, plane-parallel geometry, and include blanketing effects from the hydrogen Balmer and Lyman line series. The diffusion equation is coupled self-consistently with the usual equations describing the structure of the atmosphere: hydrostatic, radiative, and statistical equilibria, and the particle and charge conservation equations. The solution of this system of equations is obtained using an iterative method which is exact to first order: complete linearization coupled to the Feautrier elimination scheme, as described by Mihalas, Auer, & Heasley (1975). The He to H ratio at each depth is updated at each iteration by solving the diffusion equation relative to the mass scale. In § 2.1 we describe the solution of the diffusion equation, and in § 2.2 we examine some details of the radiative transfer equation pertinent to stratified atmospheres. We present the model grid in § 2.3, and we briefly examine the problem of convection in these models in § 2.4.

2.1. *Chemical Abundance Profile*

Early attempts to describe a nonhomogeneous distribution of an atomic element in a model atmosphere calculation were severely limited by the apparently simple but numerically problematic assumption of a discontinuous transition between chemically distinct layers (Heise & Huizenga 1980; Muchmore 1982). Following a method used in calculations of envelopes in diffusive equilibrium (Arcoragi & Fontaine 1980; Dziembowski & Koester 1981), Jordan & Koester (1986) published a set of H/He stratified model atmospheres with relatively thin hydrogen layers. The description of the transition zone between the overlying H-rich layers and the He-rich envelope can be done in a fully physical fashion, using the solution of the static diffusion equation at equilibrium, provided the medium is convectively stable. This transition zone is relatively broad and will prove to be numerically easy to handle provided that the independent variable is Lagrangian, and that the convergence procedure of the code secures a rigorous total flux constancy at each depth.

The equilibrium abundance profile of two constituents (H and He here) is primarily described by the partial pressure equations with the electric field constrained by charge neutrality. The abundance profile is thus derived from first principles. The abundance ratio $y = P_{\rm H}/P_{\rm He}$ is obtained relative to the total gas pressure $x = \ln P_g$ through the equation

$$\frac{dy}{dx} = \frac{-y[6y + 3(\gamma + 1)]}{y + 4} + \frac{y(\gamma - 1)(2y + \gamma + 1)}{2y + \gamma(\gamma + 1)} \times \left[\frac{y + 4\gamma}{y + 4} + \frac{\gamma}{2y + \gamma + 1}\frac{d\ln\gamma}{dx}\right]. \quad (1)$$

Here we assume that hydrogen is entirely ionized and that the average charge of helium is γ. Equation (1) is entirely consistent with the corresponding one found in Jordan & Koester (1986), provided brackets are added to their relation, as shown above. A more general expression can be found in Vennes et al. (1988). We may simplify further this relation by noting that the term implying the derivative of γ with respect to r is usually very small in the transition region. Moreover this relation for dy/dx can be integrated analytically for γ = constant and we present the solutions for two important specific cases, $\gamma = 1$, and $\gamma = 2$. The mean ionic charge of the helium atom in the photosphere of a white dwarf is usually higher than 1 for effective temperatures higher than 20,000 K, thus these two cases will define realistically the shape of the transition zone. Because it is a more common formulation, we use the inverse variable $y' = y^{-1} = P_{\rm He}/P_{\rm H}$. For $\gamma = 1$ the solution of equation (1), with the arbitrary condition that $x' = e^x = 1$ for $y' = 1$ (i.e., $P_g = P_{g0}$), is

$$x' = \frac{1}{\sqrt{2}}(y' + 1)^{1/2}y'^{1/6}, \quad (2)$$

and for $\gamma = 2$

$$x' = \frac{1}{5}(9y')^{1/5}(3y' + 2)(2y' + 1)^{-2/5}. \quad (3)$$

In Figure 1, the relations (2) and (3) are drawn for x' spanning

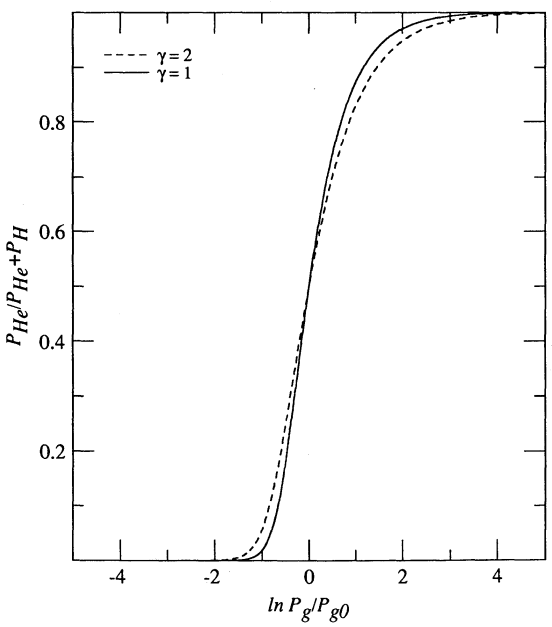

FIG. 1.—Gas pressure of helium relative to the combined hydrogen and helium pressures in terms of the total pressure ($P_e + P_{\rm H} + P_{\rm He}$) scale. This universal profile is normalized to an arbitrary pressure P_{g0} and depends only on the choice of the average ionization fraction of helium $\gamma = 1$ or 2. Hydrogen is assumed to be entirely ionized.

the transition zone. One important property of these profiles is that they share the Lagrangian property with the gas pressure P_g and, by extension, with the mass loading, m(g cm^{-2}). The gas pressure is essentially Lagrangian in our model atmosphere calculations because it depends only mildly on the physical state of the atmosphere, and strongly on the constant surface gravity, g, in the *hydrostatic equilibrium equation*:

$$\frac{dP_g}{dm} = g - g_{\rm rad} \cdot \tag{4}$$

Because $g_{\rm rad}$ is usually small (unless the white dwarf is close to the Eddington limit) the relation $P_g \approx gm$, is valid, making it easy to include a variable He/H ratio in a model atmosphere calculation, provided the choice of the independent variable is the mass loading, m. We finally need to estimate the total mass of hydrogen included in a model atmosphere, knowing, for instance, the normalization constant P_{g0}, of the variable x defined earlier. The total mass is defined to be

$$M_{\rm H} = 4\pi m_p \int_0^R r^2 n({\rm H}) dr \,, \tag{5}$$

where R is the surface radius of the star and n(H) is the hydrogen particle density (cm^{-3}). Because all hydrogen is contained within the atmospheric layers the integration is performed in practice at nearly constant radius. If we integrate equation (5) on the m scale instead of the r scale we get

$$M_{\rm H} = 4\pi R^2 \int_0^{m_\gg} \frac{dm}{1 + 4y(m)} \,, \tag{6}$$

where $m_\gg$ is taken large enough so that all hydrogen is accounted for all practical purposes. This expression can be finally expressed in terms of basic stellar atmosphere parameters, without any assumption about other physical properties of the star, by replacing the radius R with the surface gravity, g. We finally obtain

$$\frac{M_{\rm H}}{M_*} = \frac{4\pi G}{g} \int_0^{m_\gg} \frac{dm}{1 + 4y(m)} \,, \tag{7}$$

where M_* is the mass of the star. The numerical integration of this relation, for the profiles normalized so that $y(m_0) = 1$ where $m_0 = P_{g0}/g$, for $\gamma = 1$ and 2 gives

$$\frac{M_{\rm H}}{M_*} = \frac{4\pi G}{g} m_0 \quad (\gamma = 1) \tag{8}$$

$$\frac{M_{\rm H}}{M_*} = 1.3 \frac{4\pi G}{g} m_0 \quad (\gamma = 2) \tag{9}$$

In the production of a stratified model atmosphere of a given total mass of hydrogen, we simply use the average of the relations (8) and (9), thus introducing an error on $M_{\rm H}$ not larger than 10%. The total mass of hydrogen is estimated at the very beginning of the model atmosphere calculation by setting the pivot of the transition zone $y = 1$ at a selected value $m = m_0$. The H/He abundance profile is actually obtained by numerically integrating inward the equation (1) for dy/dx, considering the local value of γ at each depth of the model.

2.2. *Solution of the Radiation Field in a Stratified Atmosphere*

The rapid transition between the H and He layers, with a large step-up of the high-energy monochromatic opacities in the transition zone (see § 3), has necessitated a modification to the finite difference formulation in order to insure a more intimate coupling between the radiative transfer equation and the radiative equilibrium equation. Written in explicit form, the *radiative transfer equation*, in plane parallel geometry, reads

$$\chi_\nu \frac{\partial H_\nu}{\partial \tau_\nu} = \frac{\partial H_\nu}{\partial z} = J_\nu(\chi_\nu - n_e \sigma_e) - \eta_\nu \,, \tag{10}$$

where H_ν is the Eddington flux, J_ν is the mean intensity, χ_ν is the opacity, η_ν is the emissivity, z is the geometrical depth, and τ_ν is the monochromatic optical depth. The symbols n_e and σ_e refer to the electron density and the Thomson cross section. By integrating over frequency, we obtain the *radiative equilibrium equation*, or flux constancy:

$$\frac{\partial H_{\rm tot}}{\partial z} = \int [J_\nu(\chi_\nu - n_e \sigma_e) - \eta_\nu] d\nu = 0 \,. \tag{11}$$

In principle the ratio $\chi_\nu/\partial\tau_\nu = 1/\partial z$ in equation (10) is independent of frequency, but numerically it depends on how $\partial\tau_\nu$ is actually calculated in the finite difference scheme. The optical depth increment at the discrete frequency ν_i is usually defined, in finite differences, over three model shells $(d - 1, d, d + 1)$:

$$2\Delta\tau_{i,d} = \left(\frac{\chi_{i,d+1}}{\rho_{d+1}} + \frac{\chi_{i,d}}{\rho_d}\right) \frac{m_{d+1} - m_d}{2} + \left(\frac{\chi_{i,d-1}}{\rho_{d-1}} + \frac{\chi_{i,d}}{\rho_d}\right) \frac{m_d - m_{d-1}}{2} \,, \tag{12}$$

where ρ_{d-1}, ρ_d, and ρ_{d+1} refer to the specific density at discrete depths $d - 1$, d, and $d + 1$, respectively. This way of defining the ratio of the monochromatic opacity to the optical depth increment, $\chi_{i,d}/\Delta\tau_{i,d}$, is obviously dependent of frequency and this may result in large discretization errors that show up as total flux errors as large as 10%. In order to eliminate this large numerical error on the flux constancy, we introduce a correction factor $\epsilon_{i,d}$ to the summation in the radiative equilibrium equation (eq. [11]). The factor may take any convenient form that will insure the strict cancellation of the numerical summation. The radiative equilibrium equation in finite difference terms is then

$$\sum_i \omega_i \epsilon_{i,d} \chi_{i,d} \frac{H_{i,d+1/2} - H_{i,d-1/2}}{\Delta\tau_{i,d}} = \sum_i \omega_i \epsilon_{i,d} [J_{i,d}(\chi_{i,d} - n_{ed}\sigma_e) - \eta_{i,d}] = 0 \,, \tag{13}$$

where $H_{i,d+1/2}$ is the monochromatic flux defined over the shells d and $d + 1$, and $H_{i,d-1/2}$ is defined over the shells d and $d - 1$. With the factor $\epsilon_{i,d}$ introduced on both sides of equation (13), the ratio $\epsilon_{i,d}\chi_{i,d}/\Delta\tau_{i,d}$ is identical to $1/\Delta z$ and can be taken out of the summation on the left-hand side. The summation on the right-hand side is weighted accordingly by $\epsilon_{i,d}\omega_i$, where ω_i is the frequency quadrature weight. The summed flux at depth $d + 1/2$ is then made strictly identical to the summed flux at depth $d - 1/2$. An alternative treatment is to take a much larger number of depths, but the number involved would be prohibitive ($\gg 100$). More details on the solution of the model atmosphere using the complete linearization technique can be found in Mihalas (1978), and Mihalas et al. (1975). An application to the stratified atmosphere problem can be found in Vennes (1988).

2.3. *The Grid of Stratified Model Atmospheres*

Following the initial estimates of Vennes et al. (1988) for the hydrogen layer thickness in hot DA white dwarf stars, we have calculated a grid of stratified model atmospheres with the appropriate value of q_H. In the vast majority of models, we have assumed the same value of gravity, $\log g = 8$, but we have also computed a few models with different surface gravity to assess the effect of a change in this parameter (see below). Figure 2 shows the values of $T_{\rm eff}$ and q_H selected up to the present time for the main grid at $\log g = 8$. This new grid is a lot more extensive than that presented in Vennes (1988) and Vennes et al. (1989b) as more models are added on a continuous basis. Models with hydrogen layer masses above $\sim 10^{-15}$ M_* are appropriate to the DA white dwarfs, models with hydrogen layer masses below $\sim 10^{-16}$ M_* at 25,000 K to the DAB white dwarfs and the models with $T_{\rm eff} \geq 50{,}000$ and $q_H \leq 10^{-15.5}$ to the DAO white dwarfs. For comparison purposes, we have also computed another grid of models using the same physics but, this time, for homogeneous chemical compositions with He/H ratios in the range 10^{-10} to 10^{-2}. Details on these models can be found in Vennes (1988).

2.4. *Convection and Diffusion in Stratified Atmospheres*

A very important aspect depicted in Figure 2 is the realization that some models develop a small helium convection zone (*circles*), and that in some cases this convection zone occurs in the H/He transition zone (*filled circles*). MacDonald & Vennes (1991) discuss the importance of the choice of the convection modeling and favor the choice of the Schwarzschild over the Ledoux criterion in the context of chemically stratified layers. The latter formalism tends to suppress the convection zone due to the effect of the molecular gradient. This effect was not obtained using a more detailed treatment of convection and the simpler Schwarzschild criterion was found to correctly predict the onset of convection. We must then consider the models with convection in the transition zone as provisional, pending a detailed treatment of the interaction between convection and diffusion in model atmospheres. This interaction has already been studied in applications of model envelopes to carbon dredge-up in DQ white dwarfs (Pelletier et al. 1986; Thejll et al. 1990) and to the DBA and DAO white dwarfs (MacDonald & Vennes 1991). On the other hand, the atmospheric structure of the models with a convection zone below the transition zone ($T_{\rm eff} = 25{,}000$ K) is described correctly except for the fact that relatively large amounts of hydrogen can be hidden in the convection zone (up to $\sim 10^{-15}$ M_*). The total mass of hydrogen in these models should then be the sum of the hydrogen in the convection zone and in the small overlying diffusive hydrogen layer.

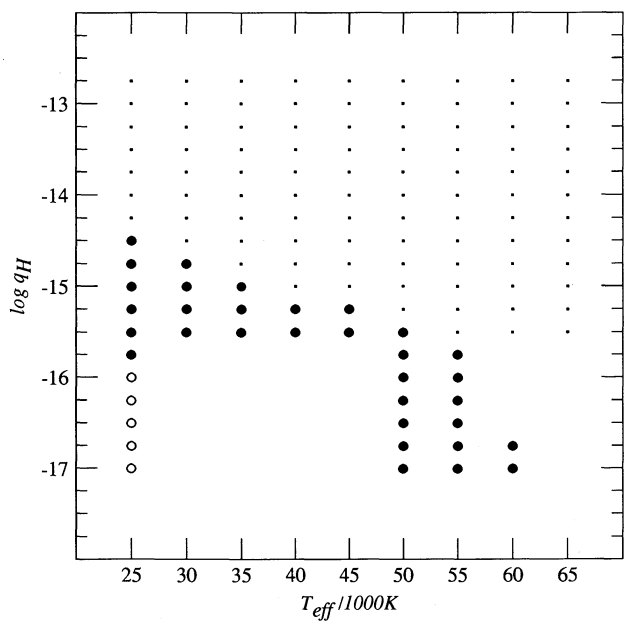

FIG. 2.—The $\log g = 8$ grid stratified model atmospheres characterized by the effective temperature $T_{\rm eff}$ and the total fractional mass of hydrogen q_H. Models developing a convection zone are represented with circles. The filled circles designate models with a convection zone in the H/He transition layers, while the open circles refer to models with a helium convection zone below the transition region.

3. SPECTRAL PROPERTIES OF STRATIFIED MODEL ATMOSPHERES

Synthetic spectra covering ranges of interest with emphasis on the EUV/soft X-ray region for the DA white dwarfs, and the optical, near- and far-UV region for the DAO and DAB white dwarfs, are calculated in full details based on the model atmosphere structures. The opacities included are the H I, He I, He II bound-bound, bound-free, and free-free transitions. The hydrogen Balmer and Lyman line series are calculated up to the series limits truncated according to the Inglis-Teller formalism. A similar approach has been adopted for the He I resonance line series and the He II ground state and excited states line series. The hydrogen line profiles Hα, Hβ, Lyα, and Lyβ are obtained from the Vidal, Cooper, & Smith (1973) tables as coded by D. Peterson and the higher members of the series are calculated following Auer & Mihalas (1972). The He I lines are treated as Voigt profiles with the Stark broadening parameters given by Dimitrijevic & Sahal-Bréchot (1984a, b). The He II ground state lines are calculated using the Auer & Mihalas (1972) formalism. The same method has been used for the $n = 2$ line series except for λ1640 which is calculated using the Schöning & Butler (1989a, b) tables of line profiles. The He II lines emerging from $n = 3$ and 4 are also calculated using the Schöning and Butler tables.

Figure 3 presents the spectral range between 50 and 1300 Å for models at $\log g = 8$ and 30,000 K (Fig. 3*a*), 40,000 K (Fig. 3*b*), 50,000 K (Fig. 3*c*), and 60,000 K (Fig. 3*d*). The hydrogen layer mass is in the range $-15 \leq \log q_H \leq -13$, a coverage typical for the analysis of the *EXOSAT* and *Einstein* data. The emergence of the helium diffusive tail in the high energy spectrum not only results in the appearance of the He II ground-state photoionization edge but also in a large suppression of the flux shortward of 227 Å when the hydrogen layer thickness is decreased. Note that the hydrogen layer is so thick in the models with $\log q_H = -13$ that those can be considered as essentially *pure hydrogen* atmospheres except for the very shortest wavelengths.

The specific spectral appearance of the stratified models presented in Figure 3 can be explained by a study of their opacity properties. The run of monochromatic optical depth, τ_ν, with mass loading, m, gives a measure of the accumulated opacity at a given wavelength and exhibits significant properties of the models. Figure 4 (*full lines*) shows the effect on the integrated opacity of variations in hydrogen layer mass for 50,000 K, $\log g = 8$, stratified models with the hydrogen fractional mass

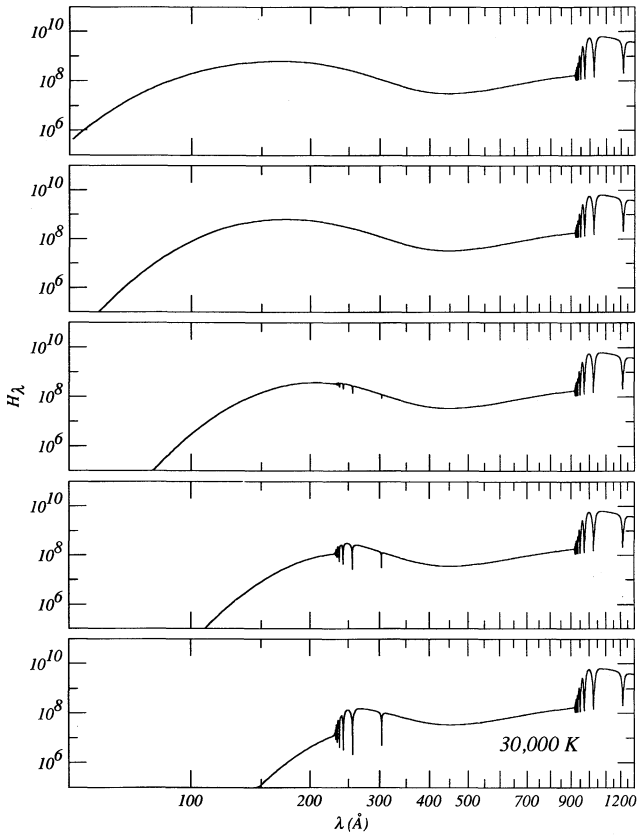

FIG. 3a

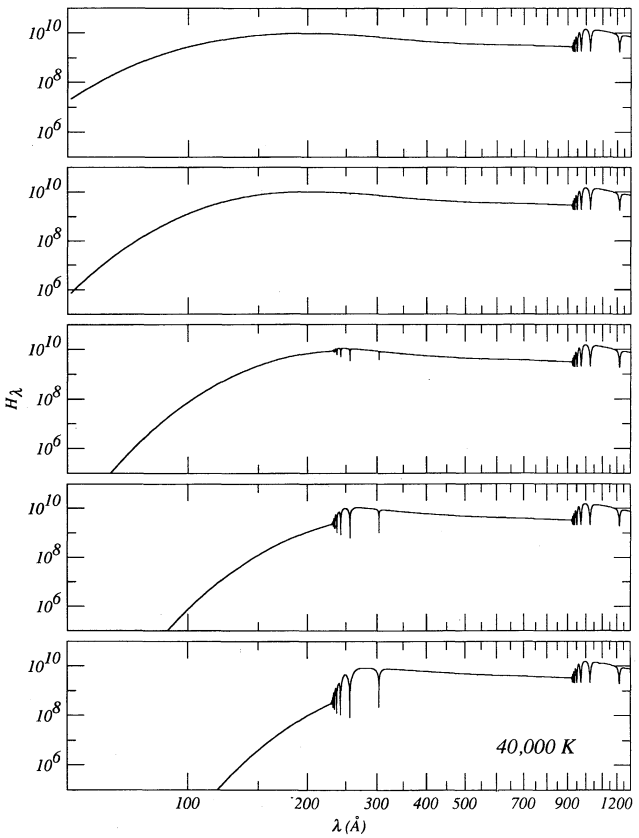

FIG. 3b

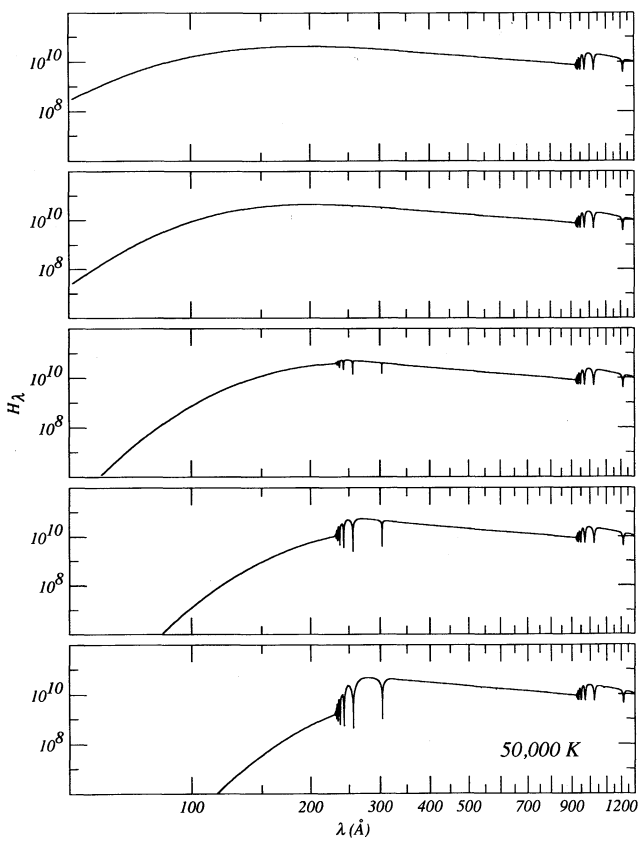

FIG. 3c

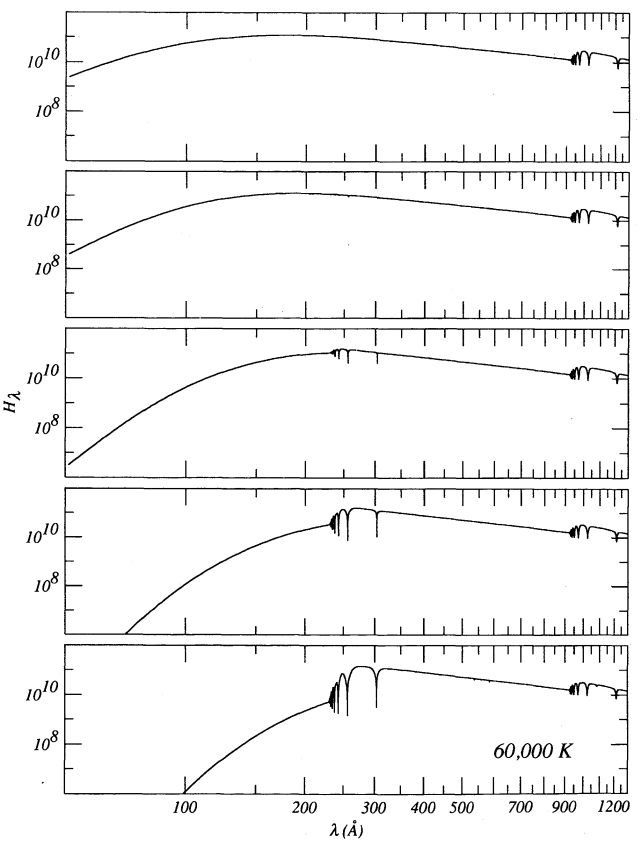

FIG. 3d

FIG. 3.—(*a*) Extreme ultraviolet spectra, H_λ (ergs cm^{-2} s^{-1} Å^{-1} sr^{-1}) vs. λ (Å), of model atmospheres at $T_{\rm eff}$ = 30,000 K, log g = 8, and from top to bottom, log $q_{\rm H}$ = −13.0, −13.5, −14.0, −14.5, −15.0. (*b*) Same as Fig. 3*a* but for $T_{\rm eff}$ = 40,000 K. (*c*) Same as Fig. 3*a* but for $T_{\rm eff}$ = 50,000 K. (*d*) Same as Fig. 3*a* but for $T_{\rm eff}$ = 60,000 K.

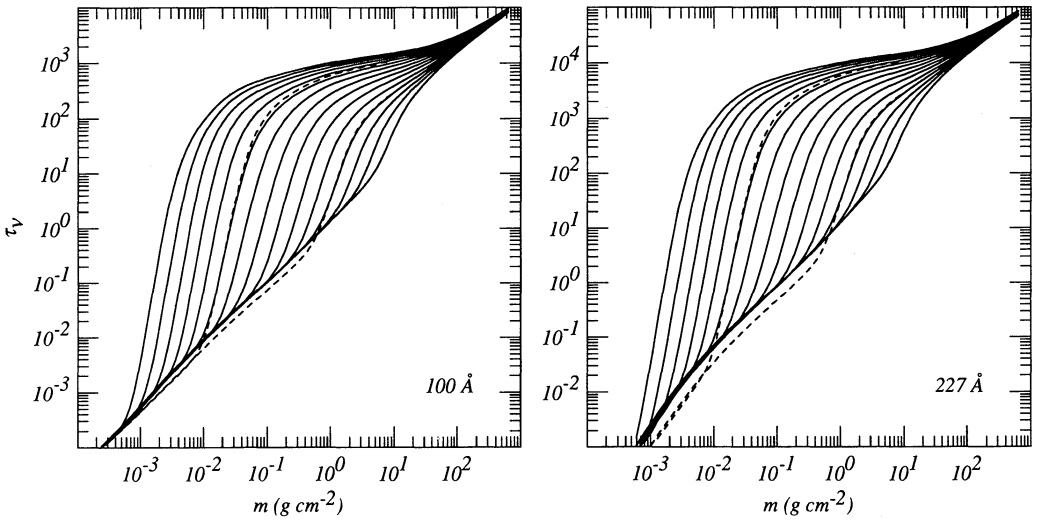

FIG. 4.—Monochromatic optical depth τ_ν at two different wavelengths ($\lambda = 100$, 227 Å) vs. mass loading scale for stratified models at $T_{\rm eff} = 50{,}000$ K, log $g = 8.0$, and $-16.25 \leq \log q_{\rm H} \leq -12.75$ (*full lines from left to right in steps of* $\Delta \log q_{\rm H} = 0.25$), and log $g = 7.5$ and log $q_{\rm H} = -13.0$, -14.5 (*dashed lines*).

in the range -16.25 (*left*) $\leq \log q_{\rm H} \leq -12.75$ (*right*) at soft X-ray (100 Å) and EUV (227 Å, below the He II, $n = 1$ photoionization edge) wavelengths. The models in Figure 4 merge to comparable opacities at depths where He dominates and in the outer layers where H dominates. Marginal differentiations at these two extremes are expected from the slightly different runs of temperature in the models with different H-layer masses. A similar phenomenon can be observed in Figure 5 which shows corresponding properties of H/He homogeneous models at the same effective temperature and gravity. As in the previous case, the curves merge to the same values at both very shallow and very deep layers. This property which applies to both stratified and homogeneous models has the same physical basis. Indeed, close to the surface and deep in the photosphere, where the material is highly ionized and dominated completely by one element, the soft X-ray opacity in all models is specified by electron scattering which is only function of electron density, a variable that varies mildly from one model to another at these extreme locations in the atmosphere.

At intermediate depths, however, Figure 4 shows that the behavior of the monochromatic optical depth is very different depending on the hydrogen layer mass. By drawing an imaginary line across the graphs at $\tau_\nu = 1$ (a representative value of the photosphere at frequency ν) we notice that a stratified model departs significantly from the pure H case (well approximated by log $q_{\rm H} = -12.75$ at this optical depth) for log $q_{\rm H} \leq -14.0$ at 227 Å, and log $q_{\rm H} \leq -13.5$ at 100 Å. In other words, EUV observations can probe for the presence of the diffusive tail of helium down to depths of log $q \approx -14.0$ in a 50,000 K, log $g = 8$ DA white dwarf, while soft X-ray observations can probe to still larger depths log $q \approx -13.5$. The greater sensitivity to hydrogen layer mass at a shorter wavelength is linked to the higher transparency of the overlying hydrogen layer at higher energy. This property shows up remarkably well in the EUV/soft X-ray synthetic spectra (Fig. 3), where a diminishing H-layer mass induces a very rapid drop of the flux shortward of the He II ground state photoionization edge. In contrast, the behavior of the homogeneous models considered here is quite different. Figure 5 shows that optical depth unity is reached at about the same atmospheric depth at 100 Å for all models with $n({\rm He})/n({\rm H}) = 10^{-10}$ to 10^{-4}. However, the right-hand side panel of Figure 5 indicates that the photosphere ($\tau_\nu = 1$) at 227 Å is located substantially higher in the star for the most heavily polluted model [$n({\rm He})/n({\rm H}) = 10^{-4}$] as compared to other models. Hence, the location of the photosphere varies more at 227 than at 100 Å in the homogeneous models, which is the exact opposite of the behavior of the stratified models. This can be understood by recalling that, for the *small* uniform traces of helium considered in the homogeneous models, the He II continuous opacity becomes nearly extinct at shorter wavelengths, which means that the location of the soft X-ray photosphere (for example) must be determined almost exclusively by the minimal opacity offered by a pure hydrogen plasma. In the stratified models, the He II continuous opacity at short wavelengths cannot be considered negligible (as in the case of homogeneous models) because the small cross-section of an individual helium atom is compensated by the higher local helium abundance which acts as a wall blocking high-energy photons coming from warmer depths.

We have also reported in Figure 4 the results of two numerical experiments in which the gravity of the models is decreased by 0.5 dex as compared to the standard models with log $g = 8$. This has some importance because Vennes et al. (1988) have called attention to the fact that variations in gravity could explain a large part of the observational scatter seen in the EUV/soft X-ray data of hot DA white dwarfs. To assess the effect of varying this parameter, we have computed two models at log $g = 7.5$ and $T_{\rm eff} = 50{,}000$ K and their opacity structures are compared to stratified models with log $g = 8$ in Figure 4: the dashed curve on the left (right) in both panels gives the behavior of the log $g = 7.5$, log $q_{\rm H} = -14.5$ (-13.0) model. Remarkably, a diminution in surface gravity is well matched by an increase in the hydrogen layer mass. For instance, the models at log $g = 7.5$ and log $q_{\rm H} = -13.0$ and -14.5 are very similar to models of the same effective temperature but with log $g = 8$ and log $q_{\rm H} = -13.5$ and -15.0, respectively.

Further properties of the stratified models are presented in Figure 6. It shows the helium abundance profiles (*continuous curves*) for models at $T_{\rm eff} = 50{,}000$ K, log $g = 8.0$, and with hydrogen layer masses ranging from log $q_{\rm H} = -16.25$ to -12.75 from top to bottom in increment of 0.25 dex. The transition zone $y = 1$, is characterized by a change in the slope

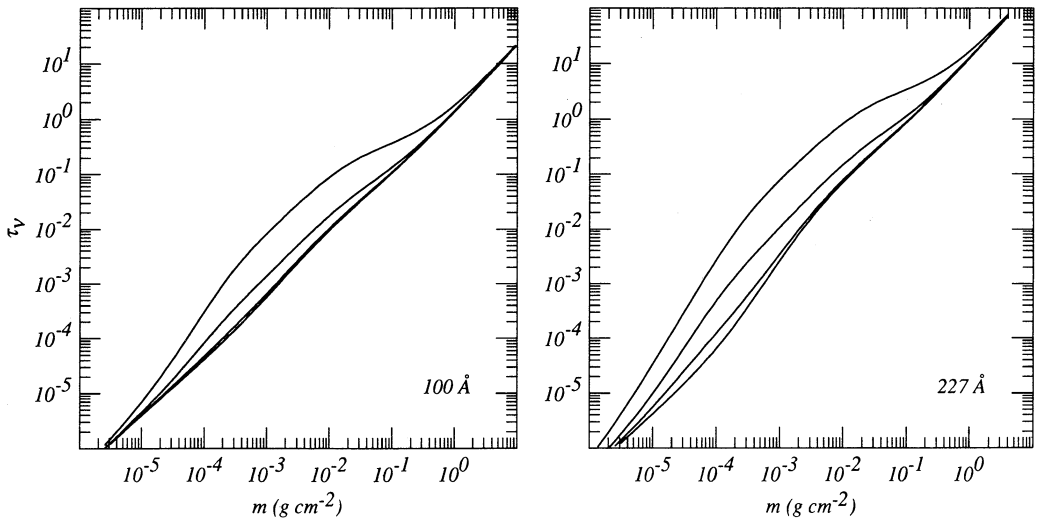

FIG. 5.—Monochromatic optical depth τ_ν at two different wavelengths (λ = 100, 227 Å) vs. mass loading scale for homogeneous models at $T_{\rm eff}$ = 50,000 K, log g = 8.0, and n(He)/n(H) = 10^{-4}, 10^{-5}, 10^{-6}, 10^{-10} from top to bottom, respectively.

(eqs. [2] and [3]) from $dy/dm = 4/5$ in a He-rich environment to $dy/dm = 5$ in a H-rich environment. The mild modulations shown in the abundance profiles in the He-rich medium are due to change in the helium ionization balance. Presented on top of the abundance profiles are the locations of the photospheres ($\tau_\nu = 1$) for three representative wavelengths in the visual (5500 Å), EUV (227 Å), and soft X-ray (100 Å) ranges as extracted from Figure 4. The comparison between the 100 and 227 Å curves demonstrates the point made earlier: the helium abundances typical of the 100 Å photosphere are much larger than the abundances found in the 227 Å photosphere. Likewise, the location of the photosphere shows a sensitivity to hydrogen layer mass down to a depth log $q \approx -14$ (-13.5) at 227 Å (100 Å). For larger hydrogen layer masses, the helium diffusive tail has receded to such large depth that it does not contribute any longer to the opacity which specifies the monochromatic photosphere. In contrast, the "visual" photosphere is largely independent of the hydrogen layer thickness in these models. Except for the thinnest models, the visual photosphere is usually located above the EUV photosphere, itself located above the soft X-ray photosphere. These results are typical of other models with different effective temperatures and correspond to the discussion presented by Vennes et al. (1988; see their Figs. 6 and 7) using approximate models.

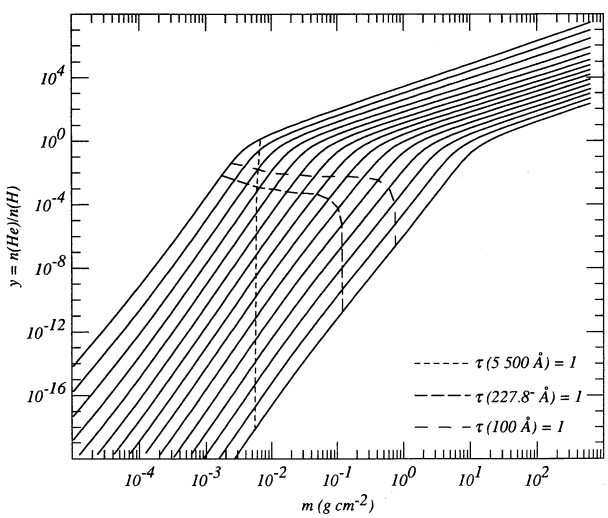

FIG. 6.—Helium abundance relative to hydrogen with respect to the mass loading scale for models at $T_{\rm eff}$ = 50,000 K, log g = 8, and, from top to bottom, log $q_{\rm H}$ = -16.25 to -12.75 by increment of 0.25 dex. The location of optical depth unity is presented for three wavelengths, one below the He II ground state photoionization edge, one in the soft X-ray, and one in the optical.

We have also used our stratified model atmospheres to compute synthetic optical spectra representative of the observed spectra of DAB and DAO white dwarfs. We consider two illustrative series of models, one at 25,000 and the other at 50,000 K, which show the emergence of the helium diffusive tail in the *optical* photosphere. In Figure 7, the most prominent helium features are He I λ4471 and λ4713, as observed in the DAB white dwarf GD 323, while the strength of the H I Balmer lines is decreasing for models with very thin hydrogen layers. Likewise, a typical DAO white dwarf spectrum can be fabricated with the emergence of He I and He II lines (particularly λ4686) in the optical spectrum for log $q_{\rm H} \leq -15.5$ (Fig. 8). The equivalent widths of selected helium UV/optical lines are presented for the two sets of models ($T_{\rm eff}$ = 25,000 and 50,000 K) in Table 1.

4. THE STRATIFIED ATMOSPHERE AS A THEORETICAL FRAMEWORK FOR THE STUDY OF HOT H-RICH WHITE DWARFS

We now consider the possibility that the spectral properties of hot H-rich white dwarfs can be explained solely in the context of stratified atmospheric layers. We focus primarily on the sample of stars observed with *EXOSAT* and *Einstein*, but we also consider the case of the DAB and DAO stars.

4.1. *Analysis of the EXOSAT Data*

The hot DA white dwarfs detected with *EXOSAT* form a sample, originally studied by Paerels & Heise (1989), of 14 stars to which were added two particularly significant nondetections and the observation of PG 1658+440 reported by Pravdo et al. (1986). This sample of *EXOSAT* targets is completed with the observations of V 471 Tau (Jensen et al. 1986), GD 2 and EG 70 (Petre & Shipman 1987), and the serendipitous detec-

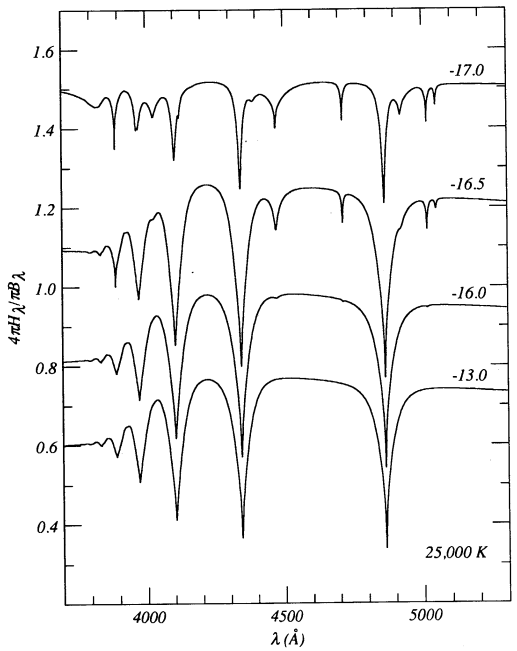

FIG. 7.—Synthetic spectra, $4H_\lambda/B_\lambda$ vs. λ, of the optical range for models at $T_{\rm eff}$ = 25,000 K and, from top to bottom, log $q_{\rm H}$ = −17.0, −16.5, −16.0, and −13.0. The synthetic spectra are shifted with an increment of 0.2 for clarity.

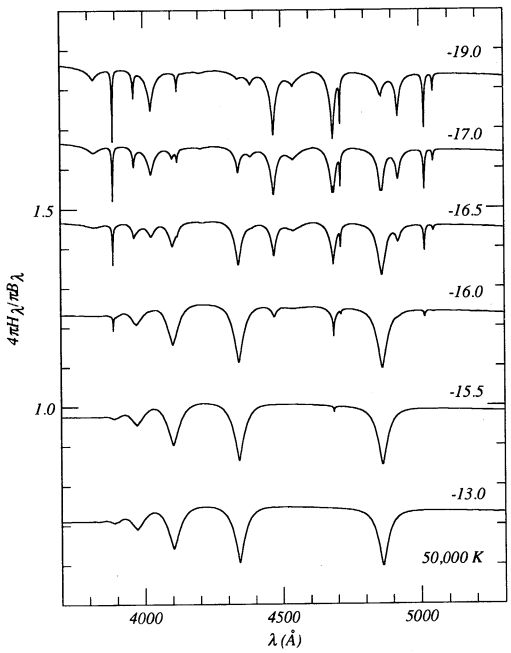

FIG. 8.—Same as Fig. 7, but for models at $T_{\rm eff}$ = 50,000 K and, from top to bottom, log $q_{\rm H}$ = −16.25, −16.00, −15.50, −14.0. The synthetic spectra are shifted with an increment of 0.2 for clarity.

tions of three more stars by Koester et al. (1990). Altogether, 23 hot DA white dwarfs were observed with *EXOSAT*. Several detections (6) of hot DA white dwarfs were also reported using the *Einstein* observatory (Kahn et al 1984; Petre et al. 1986). Of these, only GD 50 has not been observed with *EXOSAT*.

We present in Table 2 the vital statistics of all the hot DA white dwarfs observed with either *EXOSAT* or *Einstein*. To interpret the EUV/soft X-ray observations, the measured count rate in a given bandpass must be contrasted to a predicted count rate at the Earth (the procedure is explained in details in Vennes et al. 1990). The latter is proportional to the solid angle subtended by the star, and this is obtained by the ratio of the observed absolute flux given by the Johnson *V*-magnitude (or, alternatively, the Strömgren y-magnitude) to the Eddington flux of the model atmosphere at 5500 Å. Table 2 lists the magnitudes which we have used in our analysis. The model atmosphere flux in the bandpass of interest depends (in the context of layered atmospheres) on the effective temperature, the gravity, and the hydrogen layer mass. For a subsample of objects, we were able to use reliable estimates of the effective temperature and the gravity which have appeared in the literature. These estimates are based on optical photometry and UV (*IUE*) continuum fluxes complemented with Lyα line profiles measured with *IUE* in the small-aperture mode. In other cases where only rough estimates of atmopsheric parameters were available before, we have attempted (when possible) to derive more accurate values. This is important because the predicted count rates are sensitive to the atmospheric param-

TABLE 1

EQUIVALENT WIDTHS OF SELECTED HELIUM LINES

	W(Å) He II λ1640		W(Å) He I λ4471		W(Å) He II λ4686	
log $q_{\rm H}$	Δ = 15 Å	Δ = 30 Å	Δ = 15 Å	Δ = 30 Å	Δ = 15 Å	Δ = 30 Å
			A. $T_{\rm eff}$ = 25,000 K			
−15.75.....	...	...	...	...	...	...
−16.00.....	...	...	0.075	0.077	...	...
−16.25.....	...	...	0.365	0.751	...	...
−16.50.....	...	...	0.953	2.023	...	...
−16.75.....	...	...	1.250	2.477	...	...
−17.00.....	...	...	0.654	1.421	...	...
			B. $T_{\rm eff}$ = 50,000 K			
−15.00.....	0.323	0.383	...	...	...	...
−15.25.....	0.764	0.953	...	...	...	...
−15.50.....	1.354	1.771	...	...	0.105	0.140
−15.75.....	1.938	2.601	0.081	0.117	0.295	0.457
−16.00.....	2.441	3.314	0.292	0.490	0.555	0.955
−16.25.....	2.851	3.883	0.586	1.039	0.799	1.485

TABLE 2

THE SAMPLE OF DA STARS OBSERVED WITH *EXOSAT* AND *Einstein*

WD	Name	V[a]	$T_{\rm eff}$ (10^3 K)	log g	References[b]	*IUE*
0004+330.....	GD 2	13.85[c]	49.0 ± 4.0	8.5	this work	SWP 28884 L S
0050−332.....	GD 659	13.37	36.5 ± 1.5	8.2	HWB; FBB	...
0232+035.....	Feige 24	12.56[d]	55.0 ± 5.0	7.2	HWB	...
0302+027.....	Feige 31[e]	14.86	~24.0	~5.0	this work	SWP 31977 L
0320−540.....	LB 1663	(14.90)[f]	32.0 ± 2.0	7.6	this work	SWP 28887 L S
0346−011.....	GD 50	14.05[g]	42.0 ± 2.0	9.0	B91; FBB	...
0347+171.....	V471 Tauri	13.64[h]	35.0 ± 2.0	8.8	this work	SWP 9790 L S
0416−551.....	...	15.40[i]	31.0 ± 1.0	(8.0)	this work	SWP 33106 L
0425+162.....	VR 16	14.03	24.0 ± 0.5	7.7	this work	SWP 33108 L
0501+527.....	G191 B2B	11.79	62.0 ± 4.0	7.6	FBB; HWB	...
0548+000.....	GD 257	14.79[c]	44.0 ± 3.0	(8.0)	this work	SWP 33194 L
0549+158.....	GD 71	13.04	33.0 ± 1.0	7.8	FBB; HWB	...
0612+177.....	G104−27	13.39	26.0 ± 0.5	8.1	HKW; VTS	...
0642−166.....	Sirius B	8.39[j]	25.0 ± 0.5	8.6	KHW	...
1031−114.....	LTT 3870	13.01	26.0 ± 0.5	8.1	VSP; FBB	...
1254+223.....	GD 153	13.37	42.0 ± 2.0	8.2	FBB; HWB	...
1314+293.....	HZ 43	(12.93)[f]	(52.0)	(8.0)	see text	...
1620−391.....	CoD−38°10980	10.99	25.0 ± 0.5	8.1	FBB; HWB	...
1658+440.....	PG	(14.70)[f]	30.0 ± 3.0	(8.0)	this work	SWP 10290 L
2000−562.....	...	15.20[i]	36.0 ± 2.0	(8.0)	this work	SWP 33107 L
2028+390.....	GD 391	13.38	25.0 ± 0.5	8.2	VTS	...
2111+498.....	GD 394	13.08	36.5 ± 1.5	8.1	FBB; HWB	...
2240−045.....	Feige 106	15.21[c]	(45.0)	(7.0)	see text	...
2309+105.....	GD 246	13.10	54.0 ± 3.0	7.6	FBB; HWB	...

[a] Magnitudes taken from McCook & Sion 1987.

[b] (B91) Bergeron et al. 1991; (FBB) Finley et al. 1990; (HKW) Holberg et al. 1990; (HWB) Holberg et al. 1986; (KHW) Kidder et al. 1989; (VSP) Vennes et al. 1990; (VTS) Vennes et al. 1991a.

[c] Magnitude from Kidder et al. 1991.

[d] Magnitude from Holberg et al. 1986.

[e] Feige 31 is most likely a hydrogen-rich sdB.

[f] See text.

[g] Magnitude from Finley, Basri, & Bowyer 1990.

[h] Magnitude from Bois, Lanning, & Mochnacki 1988.

[i] Magnitude from Koester et al. 1990.

[j] Magnitude from Holberg, Wesemael, & Hubeny 1984.

eters, particularly to the effective temperature. Hence, for nine objects, we have used *IUE* archived data in conjunction with published optical photometry to obtain improved estimates of the effective temperature and the gravity, and this is indicated in Table 2. The method we have used is described in Vennes et al. (1990). Except for Feige 31 (which is most likely a subdwarf B star), most gravities given in Table 2 do not significantly deviate from the canonical average, and we have assumed, in the analysis which follows, a constant value log $g = 8.0$. In the previous section, we have seen that a change in surface gravity can approximately be mimicked by a change in the hydrogen layer mass, and this scaling can be applied to the few individual stars with unusual gravities.

Given a (fixed) gravity and an effective temperature (taken from Table 2), the equality of the observed and predicted count rates in a given *EXOSAT* filter implies a one-to-one relationship between the hydrogen fractional mass of the star ($q_{\rm H}$) and the interstellar neutral hydrogen column density ($n_{\rm H}$) which attenuates the flux along the line of sight. The observed count rates were taken from the literature and, when not published, from the *EXOSAT* data base (at ESTEC). We have constructed, for each filter, curves of equal likelihood (1 σ) in the log $n_{\rm H}$–log $q_{\rm H}$ plane. We reproduce in Figure 9 the results of this operation for 21 objects observed with *EXOSAT* (excluding Feige 31 and Sirius B). As can be observed in Figure 9, the quality of the inference which can be made about the possibility of a stratified atmosphere varies from star to star and depends on the quality of the filter data available. In the best possible situation, data from at least three different filters must be available. If the various curves cross each other in the same region of the log $n_{\rm H}$–log $q_{\rm H}$, the possibility of a stratified atmosphere becomes acceptable. A formal solution (i.e., acceptable χ^2) then leads to the unique values of the hydrogen layer mass and the interstellar neutral hydrogen column density which best fit the data. An example of this possibility is provided by GD 153, although the observed flux deficiency is relatively mild. In contrast, such as the case of Feige 24, the filter curves may not cross each other in the same region of the log $n_{\rm H}$–log $q_{\rm H}$ plane. In that case, the possibility of a stratified atmosphere must be rejected, a conclusion already reached in the case of Feige 24 by a study of the *EXOSAT* spectroscopy for that star (Vennes et al. 1989a).

The situation is less clear when data are available from only two filters. If the curves cross each other in the log $n_{\rm H}$–log $q_{\rm H}$ plane (e.g., GD 246), then there is clearly a flux deficiency at short wavelengths. In the absence of external constraints, the data remain consistent with the possibility of a stratified atmosphere, but nothing firmer can be said. However, the likelihood of the stratified atmosphere hypothesis could increase if studies such as that carried out by VTS fail to reveal (at more or less sensitivity) the presence of heavy elements in the UV spectrum of a particular object. Conversely, if heavy element features are detected, then absorption by heavy elements becomes a more likely possibility.

If two or more curves do not cross in the log $n_{\rm H}$–log $q_{\rm H}$ plane but converge to the same value of log $n_{\rm H}$ at large value of $q_{\rm H}$

(see e.g., GD 71 and GD 257), then no photospheric absorption has been seen by the *EXOSAT* high-energy detectors, and the probed atmospheric layers consist of pure hydrogen. In such cases, only lower limits can be put on the hydrogen layer mass. If, on the other hand, data from only one filter are available (e.g., WD 0416−551), then solutions ranging from pure hydrogen atmospheres to layered atmospheres with different hydrogen layer thicknesses become possible. Some hint on the reality of the EUV/soft X-ray flux deficiency in such cases may be obtained if the pure hydrogen solution requires an implausibly high value of n_H. Finally another situation (e.g., Feige 106) arises when only *upper limits* on filter count rates are available. Again in this case, solutions ranging from pure hydrogen atmospheres to stratified atmospheres with various possible upper limits for the values of log q_H become possible.

Another point of interest is that the solutions displayed in Figure 9 are based on the best estimates of the effective temperature which we have gathered. Considering now the uncertainties in these estimates, we find situations (particularly for lower effective temperatures) where at the low end of the allowed range no extra EUV/soft X-ray opacity is needed to account for the observed flux (GD 659), while the use of the most probable value of the effective temperature indicates a EUV/soft X-ray flux deficiency. In a similar way, we also find cases where the effective temperature at the high end of the uncertainty range suggests a flux deficiency while the most probable value of the temperature does not. We will flag such situations in the discussion which follows. The only way to establish the reality of the EUV/soft X-ray flux deficiency in those cases (and hence decide between pure hydrogen models and stratified models) is to improve the determinations of the effective temperature. In the following, we present our interpretation of the *EXOSAT* observations of hot DA white dwarfs in terms of stratified atmospheres. Table 3 summarizes our main results.

0004+330 (GD 2, EG 203).—Based on a lower temperature (46,000 K), Vennes et al. (1990) determined a hydrogen layer thickness of log $q_H = -13.4$. With the present upward revision of the temperature (49,000 K), obtained after using the new V-magnitude from Kidder, Holberg, & Mason (1991), we find log $q_H = -13.55$, in agreement with Vennes et al. for that temperature. The upper limit derived by VTS for carbon and silicon are below the level of detectability in the EUV/soft X-ray range as determined by Vennes et al. This star should be considered among the group of candidates for the detection of H/He stratification in hot DA white dwarfs.

0050−332 (GD 659).—The uncertainty in the temperature determinations based on optical and ultraviolet data does not allow a unique determination of the chemical structure of this star using EUV/soft X-ray data. At the lower end of the temperature range, all data are well fitted by a pure hydrogen atmosphere, but at the upper end some trace absorbers are needed. The most probable effective temperature (37,000 K) leads to a hydrogen layer fractional mass log $q_H = -13.50$. VTS have determined upper limits for the abundances of carbon and silicon that are well below the detectable amount in the EUV/soft X-ray range. If we assume that this star has a pure hydrogen atmosphere, then the temperature is very tightly constrained by the *EXOSAT* photometry at 35,600 ± 100 K, a result consistent with Holberg, Wesemael, & Basile (1986) and Finley, Basri, & Bowyer (1990).

0232+035 (Feige 24, EG 20).—This hot DA white dwarf has a complex atmospheric structure. Radiative levitation of elements, and possibly time-dependent effects such as those caused by a weak stellar wind, appear to be important in determining the photospheric abundance of carbon, nitrogen, and silicon observed with *IUE* and possibly several other elements seen through the *EXOSAT* EUV spectrum (Paerels et al. 1986b). It has already been demonstrated by Vennes et al. (1989a) that the characteristic stratified H/He spectrum is not

TABLE 3

HYDROGEN LAYER MASS IN HOT DA WHITE DWARFS (*EXOSAT*)

WD	Name	T_{eff} (10^3 K)	log n_H (cm^{-2})	log q_H
0004+330.....	GD 2	49.0	19.8	−13.55
0050−332.....	GD 659	35.6	18.9	> −13.10
0232+035.....	Feige 24	55.0	18.4	−14.80[a]
0320−540.....	LB 1663	32.0	18.9	> −13.05
0347+171.....	V471 Tauri	35.0	18.9	−13.45
0416−551.....	...	31.3	< 19.8	> −14.50
0425+162.....	VR 16	23.6	< 18.4	> −13.30
0501+527.....	G191 B2B	62.0	18.3	−15.00[a]
0548+000.....	GD 257	44.0	19.7 − 19.8	> −13.50
0549+158.....	GD 71	32.7	18.6	> −13.10
0612+177.....	G104−27	26.0	19.0	< −14.20
			20.0	pure H
0642−166.....	Sirius B	25.0	18.5	> −13.00
1031−114.....	LTT 3870	26.0	19.0	> −13.35
1254+223.....	GD 153	42.0	18.9	−13.55
1314+293.....	HZ 43	52.0	19.0	> −13.20[b]
1620−391.....	CoD−38°10980	24.5	18.8	> −13.25
1658+440.....	PG	30.0	18.7	> −13.50
2000−562.....	...	36.0	19.5	> −13.50
2028+390.....	GD 391	25.0	19.0	> −13.35
2111+498.....	GD 394	36.0	19.1	−13.55
2240−045.....	Feige 106	45.0	19.5	< −14.40
			20.5	pure H
2309+105.....	GD 246	54.0	19.3	−13.90

[a] This solution is not formally acceptable ($\chi^2 > 3$).

[b] 3 σ error bars on the count rates.

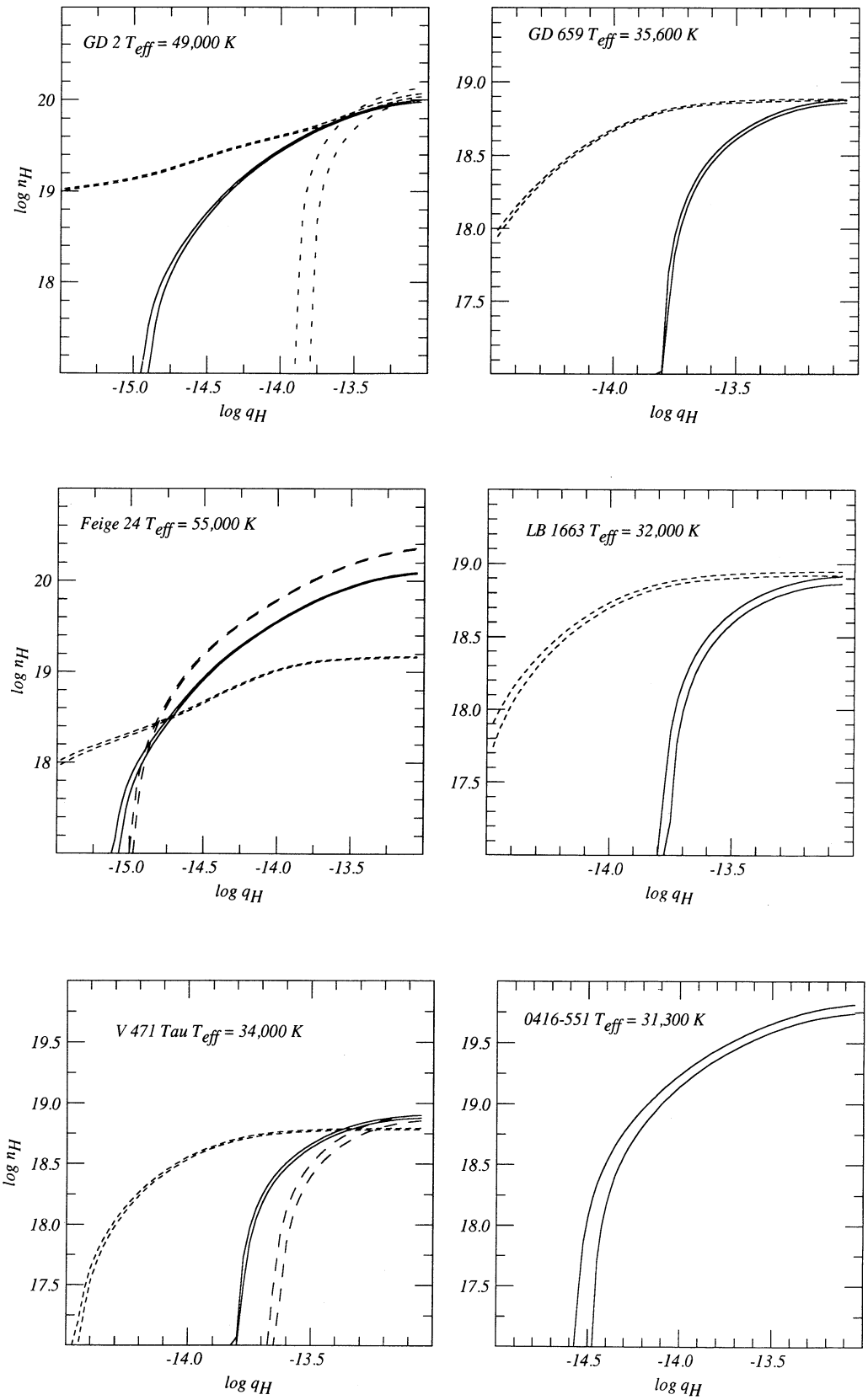

FIG. 9.—Equal likelihood curves (1 σ) for the *EXOSAT* count rates in the log n_H vs. log q_H plane for 21 hot DA white dwarfs. Each set of curves correspond to a different filter: (*solid line*) lexan 3000 Å, (*long dashed, wide spaced line*) lexan 4000 Å, (*short dashed line*) Al/P, (*long dashed line*) PPL, or (*short dashed, wide spaced line*) boron.

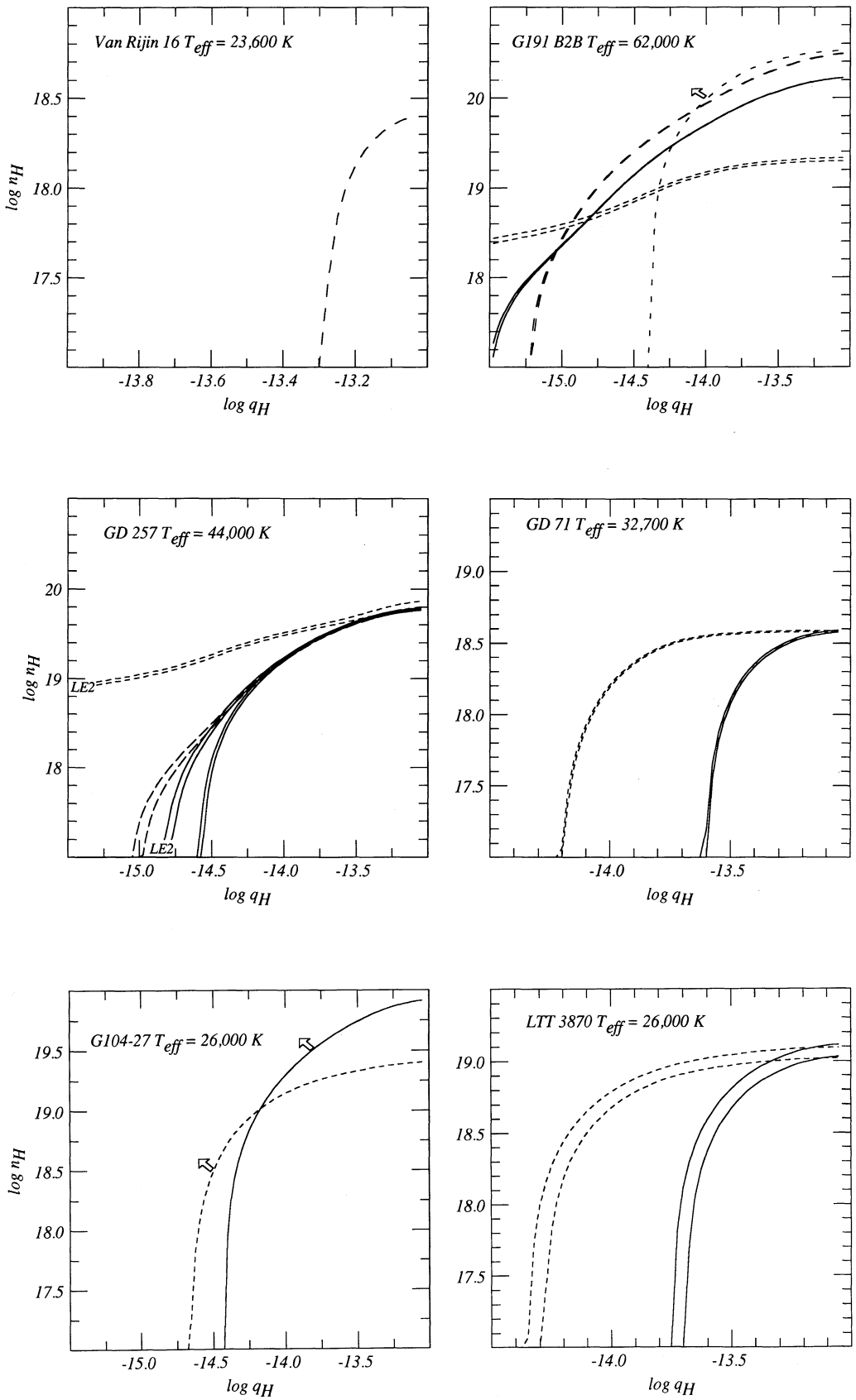

FIG. 9.—*Continued*

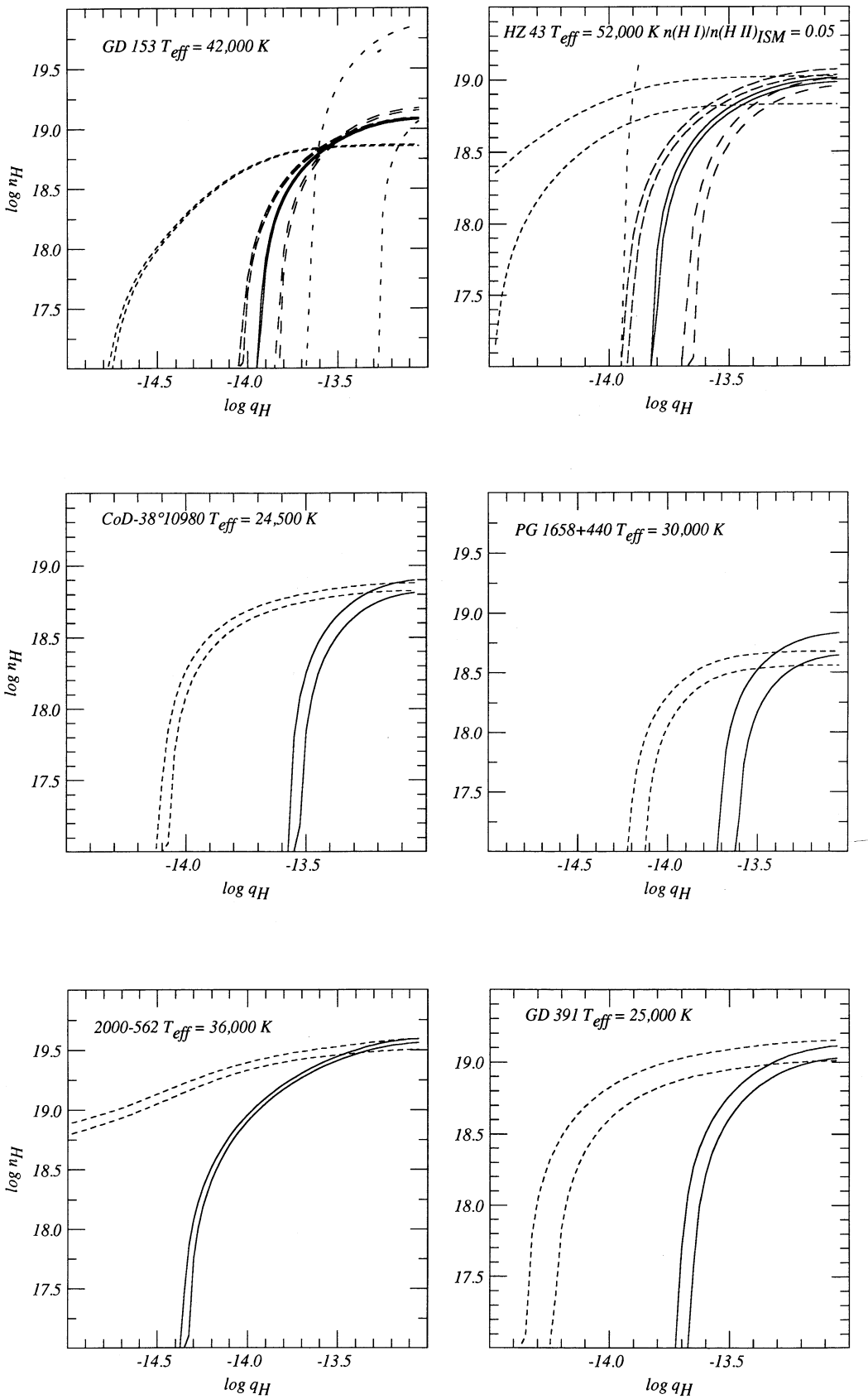

FIG. 9.—*Continued*

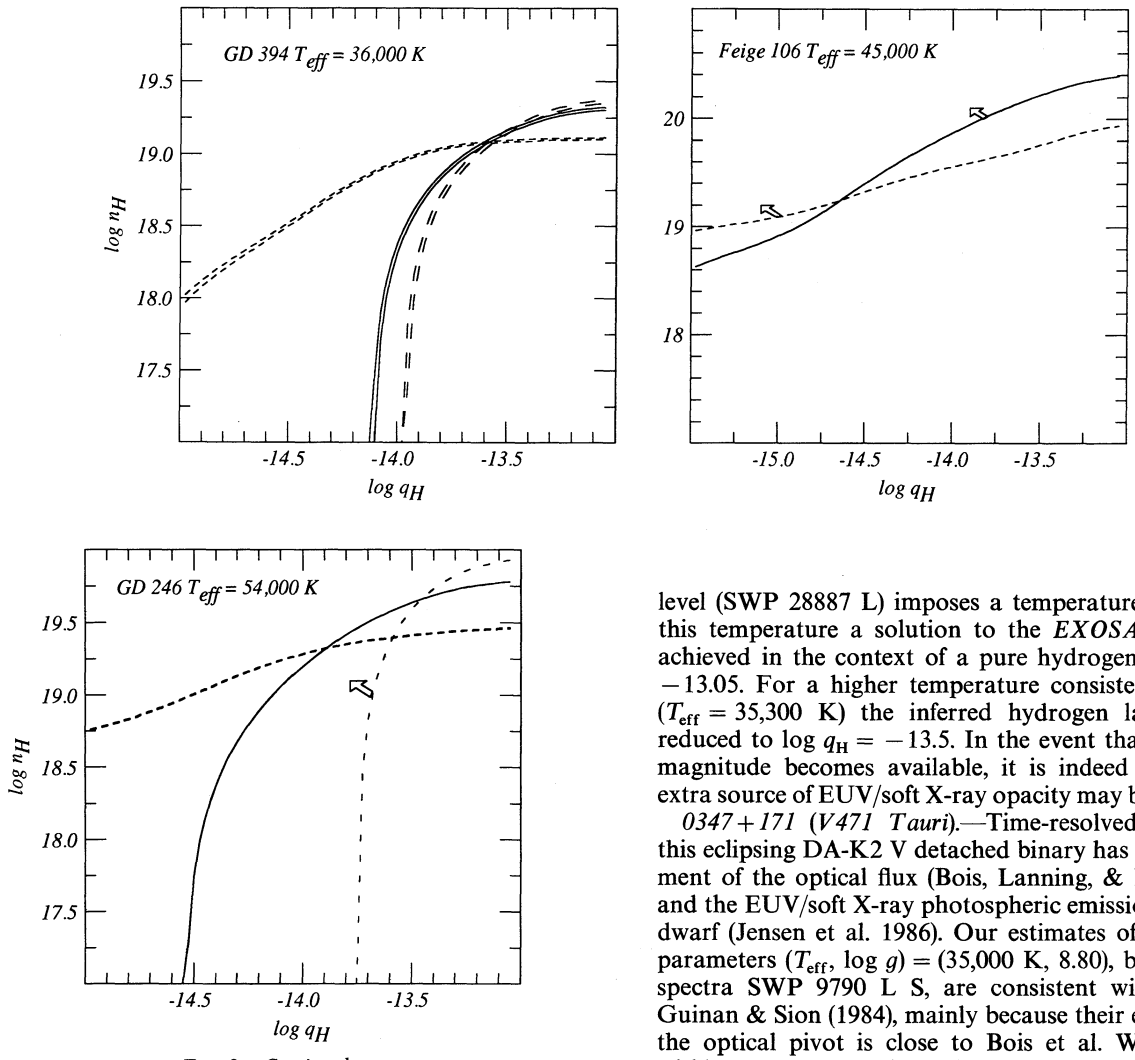

FIG. 9.—*Continued*

detected in Feige 24, so not surprisingly the *EXOSAT* photometric measurements are very poorly modeled by stratified atmospheres. The very high minimum χ^2 achieved (9.7) simply supports this conclusion based on the details of the *EXOSAT* grating spectroscopy presented by Paerels et al. This fit gives formally a value of log $q_H = -14.8$ in Table 3, but it is clearly not acceptable.

0302+207 (*Feige 31, GD 41, Gr 270*).—The gravity of this star, set by the shallow red wing of Lyα, is much lower than 10^8 cm s^{-2}. The detection of this star by *EXOSAT* is problematic since it requires at log $g = 5$ a temperature higher than 38,000 K. Ultraviolet measurements using *IUE* suggest a much lower temperature of about 24,000 K. The detection of the H-rich subdwarf Feige 31, like the DA WD 1910+047 (Margon, Bolte, & Anderson 1987; Vennes 1990), is raising the possibility that a hidden hot high-gravity white dwarf companion is responsible for the EUV/soft X-ray emission, while a cooler but lower gravity (larger radius and hence larger luminosity) star is dominating the optical/UV range.

0320−540 (*LB 1663*).—The optical pivot is very uncertain, although Kahn et al. (1984) used an optical constraint characterized by $V = 14.9$–15.0. At $V = 14.9$ the *IUE* ultraviolet flux level (SWP 28887 L) imposes a temperature of 32,000 K. At this temperature a solution to the *EXOSAT* count rates is achieved in the context of a pure hydrogen model (log $q_H > -13.05$. For a higher temperature consistent with $V = 15.0$ ($T_{eff} = 35{,}300$ K) the inferred hydrogen layer thickness is reduced to log $q_H = -13.5$. In the event that a better optical magnitude becomes available, it is indeed possible that an extra source of EUV/soft X-ray opacity may become necessary.

0347+171 (*V471 Tauri*).—Time-resolved observations of this eclipsing DA-K2 V detached binary has allowed measurement of the optical flux (Bois, Lanning, & Mochnacki 1988) and the EUV/soft X-ray photospheric emission from the white dwarf (Jensen et al. 1986). Our estimates of the atmospheric parameters (T_{eff}, log g) = (35,000 K, 8.80), based on the *IUE* spectra SWP 9790 L S, are consistent with the results of Guinan & Sion (1984), mainly because their earlier estimate of the optical pivot is close to Bois et al. With temperatures within error bars we have determined that the average count rates over one 9.25 minutes period indicate the presence of absorbers. In the context of stratified atmospheres we infer a value log $q_H = -13.45$. This is thick enough to rule out the driving mechanism discussed in Stanghellini, Starrfield, & Cox (1990) to explain the 9.25 minutes pulsation period, which requires a hydrogen layer thickness less than log $q_H = -13.9$ (at 0.8 $M_\odot$). The required temperature consistent with such a low hydrogen layer mass would exceed 40,000 K, which is ruled out from our UV temperature analysis. In any case, it has been found that the light variability in the optical (also observed in the EUV/soft X-ray range) is characteristic of the rotation of a nonhomogeneous surface rather than the g-mode pulsations observed in the DAV and DBV stars (Clemens et al. 1992). In light of this, it is possible and perhaps more likely that the inferred EUV/soft X-ray opacity is caused by accreted material on magnetic poles that managed to diffuse below the FUV photosphere. The nondetection of photospheric carbon and silicon in V471 Tau by Mullan et al. (1991) is consistent with other nondetections in DA white dwarfs of similar temperatures (VTS) but it does impose rather inefficient accretion onto this white dwarf. Whether enough material can still be accumulated down below in the EUV/soft X-ray photosphere remains to be investigated. Finally we note the anomalously large surface gravity inferred from the broad Lyα red wing and

models at 35,000 K (at 34,000 K the Lyα wing is consistent with log $g = 8.4$).

0416−551.—This very faint DA white dwarf, discovered by Koester et al. (1990), has an effective temperature based on ultraviolet flux, $T_{\rm eff} = 31{,}300$ K, that requires large suppression of the EUV/soft X-ray flux in order to explain the low lexan 3000 Å count rate. This is accomplished either with a stratified atmosphere at log $q_{\rm H} = -14.5$ if the interstellar hydrogen column is small or by a pure hydrogen model with a large column density, $n_{\rm H} = 6 \times 10^{19}$ cm^{-2}. Stratified models between the two extremes are also possible.

0425+168 (VR 16, EG 37, KUV).—Our UV-based temperature, $T_{\rm eff} = 23{,}600$ K, is in agreement with color-determined temperatures. At this temperature, the lexan 4000 Å count rate obtained by Koester et al. (1990) requires the hydrogen layer mass to be larger than $5 \times 10^{-14}\ M_*$ if the interstellar hydrogen column density is negligible. Alternatively the column density must be smaller than 2.5×10^{18} cm^{-2} if we assume a pure hydrogen composition. As in the previous case, intermediate models are also possible. Van Rhijn 16 is the coolest DA white dwarf ever detected in the EUV/soft X-ray range.

0501+527 (G191 B2B, EG 247).—This hot DA star quite possibly shares with Feige 24 similar photospheric abundances of carbon, nitrogen and silicon, and like Feige 24 has an effective temperature among the highest for the H-rich degenerates and a lower gravity than average. Moreover, Reid & Wegner (1988) and Vennes et al. (1991b) have determined that these stars have small gravitational redshifts of about 15 km s^{-1}, characteristic of white dwarfs with larger radii or smaller masses than average. The gravity determinations of Holberg et al. (1986) of log $g = 7.23$ and 7.55 for Feige 24 and G191 B2B, respectively, support this conclusion. An examination of the count rate analysis of these two stars also reveals their *extraordinary* similarity, and the failure of the stratified model is even more patent in this case ($\chi^2 = 21.6$). It is then very likely that G191 B2B has its EUV spectrum regulated by heavy element trace absorbers as shown in the case of Feige 24 by Vennes et al. (1989a), although it is not clear yet whether the effect of H/He stratification contributes or not in this case.

0548+000 (GD 257, Gr 289).—A new V magnitude (Kidder et al. 1991) and the *IUE* short-wavelength spectrum obtained by Holberg and Wesemael (SWP 33184 L), together suggest a much lower temperature, $T_{\rm eff} = 44{,}000$ K, than the 61,810 K previously estimated by Finley et al. (1990). At this temperature, GD 257 is well described by a pure hydrogen atmosphere. The previous higher temperature estimate requires the presence of EUV/soft X-ray absorbers other than hydrogen (see Vennes et al. 1989b).

0549+158 (GD 71, EG 210).—This is another case for a pure hydrogen atmosphere, based on high-dispersion ultraviolet data (VTS) and the present analysis of the *EXOSAT* photometry. The accurate EUV/soft X-ray photometry for this star is very constraining on both the trace element abundances and the effective temperature. If we propose *a priori* that this star has a pure hydrogen atmosphere, then the effective temperature is constrained to $32{,}700 \pm 100$ K.

0612+177 (G104−27, EG 46).—The detection of He I λ4471 by Holberg, Kidder, & Wesemael (1990) in high signal-to-noise spectra of G104−27 has apparently solved the mystery of the nondetection of this star by *EXOSAT*. The interstellar hydrogen column density required to totally quench the EUV/soft X-ray flux of this 26,000 K star is prohibitively high at 10^{20} cm^{-2}, although a stratified atmosphere with log $q_{\rm H} = -14.2$ would only require 10^{19} cm^{-2}. The reported equivalent width of the He I line translates into a hydrogen layer mass of log $q_{\rm H} = -16.2$ (see Table 1), but then He I λ4713 should have been detected as well. The nature of this star, tentatively classified among the small group of DAB white dwarfs, is as mysterious as for the DAB prototype GD 323 (Liebert et al. 1984). The presence of a surface He convection zone below the very thin hydrogen layer does suggest caution when estimating the hydrogen layer thickness. A large amount of hydrogen may be hidden in the convection zone. The recent discussion of Kidder et al. (1992) suggests that the presence of helium in the photosphere of G104−27 is a transient phenomenon. The star may be undergoing a mixing episode at its surface. A model with a nonuniform *horizontal* chemical composition (variable with time) may be more appropriate than a stratified atmosphere in this case. Further investigations in the EUV/soft X-ray range aimed at detecting G104−27 are clearly warranted.

0642−166 (Sirius B).—The fascinating story of Sirius B has truly made this star the prototype of the X-ray emitting hot DA white dwarfs. Indeed the debate concerning the source of the high-energy emission between two models, photospheric (Shipman 1976) or coronal emission (Hearn & Mewe 1976), was focused on this object. The current status of this star based on FUV and EUV spectroscopy (Paerels et al. 1988; Kidder, Holberg, & Wesemael 1989) is $T_{\rm eff} = 25{,}000$ K log $g = 8.6$, $R/R_\odot = 0.0085$–0.0095, with a pure H atmosphere. Our interpretation of the integrated spectra presented by Paerels et al., using a sequence of pure hydrogen models at log $g = 8.5$, gives a solution ($T_{\rm eff}$, log $n_{\rm H}$) = (25,000 K, 18.5) and $R/R_\odot = 0.0086$. These results are consistent with Paerels et al. and Kidder et al. If the temperature is set very precisely from the count rate analysis, then the hydrogen layer mass is constrained to log $q_{\rm H} \geq -13$.

1031−114 (LTT 3870, EG 70).—Vennes et al. (1990) have explained all observations of this star in terms of a pure hydrogen atmosphere. Moreover VTS have determined that neither carbon or silicon is detected in the photosphere of this star.

1254+223 (GD 153, EG 187).—The effective temperature of GD 153 has been accurately determined both from optical and *IUE* ultraviolet measurements. The result of the count rate analysis reveals the presence of a source of EUV/soft X-ray opacity. The remarkable fact is that the study of the *IUE* high-dispersion spectra by VTS failed to reveal any trace of carbon, nitrogen or silicon with upper limits that exclude any influence of these heavy elements on the high-energy spectrum of that star. We are therefore left with a conclusion similar to that for GD 2: the high energy spectrum of GD 153 may show that presence of a thin hydrogen layer. Our estimate of the appropriate hydrogen layer mass is log $q_{\rm H} = -13.55$.

1314+293 (HZ 43, EG 98).—The *EXOSAT* spectroscopic observations reported by Paerels et al. (1986a) and reanalyzed by Heise et al. (1988) have cast some doubts on whether HZ 43 is a reliable standard candle light source. The formal solution obtained at $T_{\rm eff} = 60{,}000$ K was setting a stellar radius from the EUV/soft X-ray measurement a factor of 2 smaller than from UV measurements (Holberg et al. 1986). Only at 50–54×10^3 K do the radius estimates agreed, but this was at the expense of the statistical acceptability of the model atmosphere fit to the *EXOSAT* spectroscopy. Moreover the V-magnitude derived by Holberg et al. would have to be reduced by 0.06 mag to $V = 12.93$. We offer one more piece of evidence that

something is wrong with the current modeling of HZ 43. *There is no formal solution to the EXOSAT photometry within 1 σ error bars* (see Fig. 9). None of our basic physical assumptions has the potential of resolving the discrepancy. Using 3 σ error bars on all photometric measurements, a satisfactory solution ($\chi^2 = 1.9$) is obtained at 52,000 K, $\log q_H > -13.1$, and $\log n_H = 19.0$. In this analysis we have arbitrarily set the ratio of the neutral hydrogen to the total hydrogen in the ISM to 5%, bringing our measured $n_{H\,I}$ to 5×10^{17} cm^{-2} in accord with the *Voyager* result (Holberg et al. 1980). It is not clear yet whether the current *EXOSAT* LE calibration (Parerels et al. 1990) allows such a large uncertainty in the photometric measurements. Uncertainty in the CMA detector efficiency is probably dominating the overall calibration problem. Recent attempts to reconcile the EUV/soft X-ray spectroscopic data (Parerels et al. 1986a) with complementary data in the optical and UV (*IUE*) failed even after allowing for uncertainty in the *EXOSAT* calibration. Only marginal improvements were obtained with the stratified H/He model atmospheres (Paerels & Vennes 1990, private communication).

1620−391 (CoD−38°10980, Gr 274).—The study of this bright object in the UV range with the *IUE* high-dispersion mode revealed the presence of ionized silicon in the line of sight (Holberg et al. 1985). No other elements have been detected. Carbon, for instance, would have been detectable through a UV C II transition (VTS). The count rate analysis places this star among the group of pure hydrogen emitters, underlining the fact that the circumstellar Si II and Si III atoms have no apparent effect on the EUV/soft X-ray flux.

1658+440 (PG).—Identified by Liebert et al. (1983) as a 3.5 MG magnetic DA white dwarf, this object was detected with *EXOSAT* and *Einstein*. Pravdo et al. (1986) found that the EUV/soft X-ray flux was consistent with a pure hydrogen atmosphere at 30,000 K. The optical pivot is somewhat difficult to set. Liebert et al. have acknowledged that the multichannel spectrophotometry was somewhat affected by Earth's atmosphere obscuration and they assumed a "gray" correction that brings the V-magnitude to about $V = 14.6$. The resulting temperature $T_{\rm eff} = 28{,}000$ K is too cool for the measured *EXOSAT* count rates. We have set the magnitude at $V = 14.7$, resulting in a temperature of 30,000 K. We then find that the *EXOSAT* photometry is consistent with a pure hydrogen atmosphere.

2000−562.—The second hot DA white dwarf discovered serendipitously by Koester et al. (1990), this object may show at $T_{\rm eff} = 40{,}000$ K, the presence of a thin hydrogen layer ($\log q_H = -13.55$) although formally all solutions are acceptable for $\log q_H \geq -13.7$. Our ultraviolet-based temperature, $T_{\rm eff} = 36{,}000$ K, suggests a pure hydrogen configuration, $\log q_H \geq -13.50$.

2028+390 (GD 391, EG 243, Gr 397).—With GD 71, Sirius B, LTT 3870, HZ 43, and CoD−38°10980 (possibly GD 659) this DA is among the group of pure hydrogen white dwarfs, that do not show the presence of photospheric trace elements in the FUV or EUV/soft X-ray ranges (VTS). To this group we could perhaps add GD 257, PG 1658+440, and LB 1663 but the absence of *IUE* high-dispersion spectroscopy or the uncertainty of their effective temperatures do not allow firm conclusions to be drawn. Our lower limit on the hydrogen layer mass in GD 391 is $\log q_H > -13.35$.

2111+498 (GD 394, EG 244, Gr 399).—The rather secure effective temperature and gravity for this star used in conjunction with the *EXOSAT* data impose the presence of a source of EUV/soft X-ray opacity. The count rate analysis results in a hydrogen layer thickness $\log q_H = -13.55$. Only at a significantly improbable temperature of about 33,700 K do the count rates match the prediction of a pure hydrogen atmosphere. GD 394 has been identified by Bruhweiler & Kondo (1983) as a possible candidate for the presence of stellar winds in white dwarfs. The ultraviolet spectrum shows blueshifted Si III and Si IV lines that may originate from a halo expanding at ~30–50 km s^{-1}. The presence of ionized material, possibly in a circumstellar halo in the present case, may affect the interpretation of the EUV/soft X-ray spectrum although carbon is notably absent from the UV spectrum, as in CoD−38°10980.

2240−045 (PHL 380, Feige 106, GD 240, EG 229).—There are no precise atmospheric parameters available for this star. Kidder et al. (1991) have classified this object as a DA white dwarf and *UBV* photometry places this object in the vicinity of known hot DA white dwarfs in the $(U-B, B-V)$ two-color diagram: GD 2, GD 257, and the DAO PG 1210+533. We estimate the effective temperature to be between 40,000 and 50,000 K with a gravity possibly smaller than average ($\log g \approx 7$). Using $T_{\rm eff} = 45{,}000$ K, the upper limits on the *EXOSAT* count rates would require $\log q_H = -14.4$ if one assumes $\log n_H > 19.5$.

2309+105 (GD 246, EG 233, BPM 97895).—The count rate analysis reveals the undisputable presence of EUV/soft X-ray absorbers, and yet the VTS analysis of the *IUE* high-dispersion data failed to detect C, N, or Si. However, in an independent analysis, Jelinsky (1988) has assigned equivalent widths to possible C IV and Si IV lines, consistent with VTS upper limits. The equivalent abundances of these elements alone would be insufficient to strongly affect the EUV/soft X-ray flux. Along with GD 2, GD 153, and GD 394, GD 246 is thus another DA which may have a thin hydrogen layer. We estimate that $\log q_H \approx -13.90$.

In summary, our analysis of the *EXOSAT* sample reveals that in at least four stars (GD 2, GD 153, GD 394, and GD 246) the hypothesis of a stratified atmosphere as the main explanation for the observed EUV/soft X-ray flux deficiency is a viable one. In contrast, this idea must be rejected in two objects (Feige 24, G191 B2B). In addition, the spectral properties of eight stars (GD 257, GD 71, Sirius B, LTT 3870, HZ 43, CoD−38°10980, PG 1658+440, and GD 391) can be accounted for solely on the basis of pure hydrogen atmospheres. For some of the remaining stars, we cannot decide yet on the reality of the EUV/soft X-ray flux deficiency and, therefore, on the choice of pure hydrogen atmospheres *versus* stratified models. For instance, using the most probable effective temperature for LB 1663 and WD 2000−562, we find that the observed short-wavelength fluxes are compatible with the emission of a pure hydrogen atmosphere. However, using values of the effective temperature at the high end of the uncertainty range, we find a flux deficiency in both stars. Similarly, if we take our adopted value of the effective temperature for GD 659, an extra opacity source is required, while a more transparent pure hydrogen atmosphere is sufficient if we use a lower value of the effective temperature which is still within the error bars. Better determination of the effective temperature are required for those three objects. Insufficient filter data (either only one bandpass available or upper limits) for WD 0416−551, VR 16, and Feige 106 (in addition to uncertain atmospheric parameters in the latter case) also precludes us from deciding between pure hydrogen atmospheres and stratified models. Finally, two other stars remain unusual. We have

obtained a good fit to a stratified atmospheric structure for V471 Tau, but it remains unclear how to relate that to the properties of this white dwarf which is a member of a rather complex binary system. We cannot certainly rule out the hypothesis of a stratified atmosphere in this star, but it remains to be seen how this can be made compatible with the possibility of accretion on the poles. The case of G104−27 presents new possibilities for atmospheric structures: the nonuniform and possibly time dependent surface (H/He) chemical composition is possibly horizontal rather than vertical, so our stratified model atmospheres in diffusive equilibrium probably do not apply.

A final remark is concerned with the apparent discrepancy between the interstellar neutral hydrogen column density inferred here with *EXOSAT* data and the column density derived from *Voyager* EUV flux measurements (Holberg 1984). Three hot DA stars, G191 B2B, GD 153, and HZ 43, with respectively $n_{\rm H\,I} = 1 \times 10^{18}$, 6×10^{17}, and 4×10^{17} cm^{-2} were detected by *Voyager* and are in common with our *EXOSAT* sample (see Table 3). Our inferred values of $n_{\rm H}$ are significantly larger for GD 153 and HZ 43. This discrepancy arises from the fact that *Voyager* offers a *direct* measurement of the neutral hydrogen while *EXOSAT* gives a *scaled* measurement of the neutral hydrogen. At soft X-ray wavelengths typical of *EXOSAT*, neutral helium is the dominant interstellar opacity source, so that a comparison of these two estimates of the neutral interstellar hydrogen column density is in fact a measurement of the ratio of neutral helium to neutral hydrogen. Since the cosmic abundance ratio is not likely to vary much from one object to another, the physical effect involved here is most probably variable partial ionization of hydrogen in various lines of sight. For HZ 43 and GD 153, the ionization ratio n(H II)/n(H I) is likely to be greater than 90%, while for G191 B2B it is less than 50%, a result confirmed by Green, Jelinsky, & Bowyer (1990). Specific circumstances lead to this conjuncture: G191 B2B probably does not lie in the midst of previously ionized gas and, being the hottest white dwarf of the three, it is much younger and hence has not had enough time to partly ionize the surrounding ISM.

4.2. *Analysis of the Einstein Data*

In the following, we consider the *Einstein* observations of LB 1663, GD 50, GD 257, GD 153, and PG 1658+440 with the IPC detector, and we model as well the HRI count rate of GD 246. Of these, only GD 50 was not observed with *EXOSAT*. We consider also HZ 43 and Sirius B which have been observed with both the IPC and HRI detectors. The latter objects are used in particular in a comparison between the *EXOSAT* and *Einstein* data. The IPC count rates have been taken from Kahn et al. (1984), Pravdo et al. (1986), and J. Schachter (The *Einstein* IPC Slew Survey 1990, private communication). The HRI count rates were taken from Vaiana et al. (1981) and Petre et al. (1986). The results of our analysis for six objects are summarized in Table 4. The effective temperatures are those given in Table 2. Since there is only one bandpass available for each star, we have used the estimates of the interstellar neutral hydrogen column density derived from the analysis of the *EXOSAT* data (which are very sensitive to this parameter) for the five objects in common in both samples. This allows a determination of the hydrogen layer mass in the context of stratified atmospheres. Details on the individual objects follow.

TABLE 4

HYDROGEN LAYER MASS DETERMINATION IN HOT DA WHITE DWARFS (*Einstein*)

WD	Name	$T_{\rm eff}$ (10^3 K)	log $n_{\rm H}$ (cm^{-2})	log $q_{\rm H}$
0320−540.....	LB 1663	32.0	18.9	−13.40
0346−011.....	GD 50	43.0	< 19.0	−13.55–13.65
0548+000.....	GD 257	44.0	19.8	−13.50
1254+223.....	GD 153	42.0	18.9	−13.40
1658+440.....	PG	30.0	18.7	−13.50
2309+105.....	GD 246	54.0	19.3	−13.85

0320−540 (LB 1663).—The hydrogen layer thickness (log $q_{\rm H} = -13.40$) inferred from the IPC count rate using the hydrogen interstellar column density from the *EXOSAT* analysis does indicate the presence of trace absorbers, in contradiction with the *EXOSAT* result. We recall, however, that the uncertainties in $T_{\rm eff}$ for LB 1663 are sufficiently large that the *EXOSAT* results are not completely incompatible with the presence of some photospheric absorption (see above). Alternatively, if we use the upper limit on the hydrogen layer thickness from *EXOSAT* the inferred neutral hydrogen column density from the IPC measurement is much larger, log $n_{\rm H} = 19.6$, than estimated previously. A unique solution ($\chi^2 = 1.8$) to both *EXOSAT* and *Einstein* observations is obtained only for the temperature $T_{\rm eff} = 35{,}000$ K and (log $q_{\rm H}$, log $n_{\rm H}$) = (−13.5, 19.1). The effect of including the IPC count rate in the analysis is then to increase the temperature and to reveal a thin hydrogen layer.

0346−011 (GD 50).—The only available datum is the *Einstein* IPC count rate, and it reveals the presence of a thin hydrogen layer (log $q_{\rm H} = -13.6$) *if* an upper limit, $n_{\rm H} \leq 10^{19}$ cm^{-2}, is assumed. In their analysis of the *IUE* high-dispersion spectra, VTS found no evidence for heavy elements in the photosphere of GD 50 suggesting the possibility that this star may have a thin hydrogen layer. More EUV/soft X-ray data are clearly needed in this case.

0548+000 (GD 257).—A situation similar to LB 1663 arises, in which the IPC seems to impose some EUV/soft X-ray absorbers, although a solution to the *EXOSAT* count rates was achieved with pure hydrogen models. The temperature that would provide a unique solution (requiring a stratified atmosphere) covers a very broad range starting from 45,000 K and higher. However our preferred temperature of $T_{\rm eff} =$ 44,000 K leads to log $q_{\rm H} = -13.5$ using the IPC.

1254+223 (GD 153).—Opposite to LB 1663 and GD 257, the IPC count rate forces in this case a hydrogen layer thickness somewhat larger than from the *EXOSAT* data alone (log $q_{\rm H} = -13.40$ compared to -13.55). Since the solution to the *EXOSAT* data is statistically very good, we have to postulate that either an unmodeled effect is shaping the observed spectrum at IPC energies or that large uncertainties are affecting the IPC measurement of extremely soft sources.

1658+440 (PG).—As in the case of GD 257, the IPC count rate suggests the presence of some short-wavelength absorption, whereas the *EXOSAT* measurements are explained in terms of a pure hydrogen atmosphere. The inferred hydrogen layer mass is log $q_{\rm H} = -13.50$.

2309+105 (GD 246).—If we adopt again the parameters ($T_{\rm eff}$ and $n_{\rm H}$) from the *EXOSAT* analysis we obtain with the HRI count rate a hydrogen layer mass log $q_{\rm H} = -13.85$. This is only 10% larger than the value obtained in the *EXOSAT* analysis. Hence, contrary to the IPC measurements, it appears

that the HRI observations show consistency with the *EXOSAT* data (at least in this case). The *EXOSAT* analysis confirms the conclusion of Petre et al. (1986) based on *Einstein* HRI data concerning the presence of EUV/soft X-ray absorbers.

It is remarkable that the *Einstein* IPC data do not corroborate in a straightforward manner the results from the *EXOSAT* data. This is not completely unexpected, however, because the *absolute* calibrations of both telescopes may differ by as much as 50%, although it is believed that the relative response of the CMA aboard *EXOSAT* is well known. We expect then that the count rate analysis of the *EXOSAT* filters to be internally consistent. One other potential problem is that the *EXOSAT* and *Einstein* detectors are relatively decoupled in terms of their energy windows, the *Einstein* IPC being sensitive at significantly shorter wavelength (peaking at $\lambda \leq 80$ Å) than the various bandpasses of *EXOSAT* (lx3: $\lambda \approx 120$ Å; Al/P: $\lambda \approx 180$ Å). The results from the *EXOSAT* data must be considered more reliable since the filter bandpasses are mapping the peak of EUV/soft X-ray emission from the hot DA white dwarfs, while *Einstein* covers the declining high-energy tail of the spectrum.

It is interesting to compare the results of *EXOSAT* and *Einstein* for HZ 43 and Sirius B. In the latter case, the *EXOSAT* EUV spectrum is perfectly consistent with a pure hydrogen atmosphere, and the atmospheric parameters are well-known. Using the value $T_{\rm eff} = 25{,}000$ K, $\log g = 8.5$, and $\log n_{\rm H} = 18.5$ (the latter derived in our *EXOSAT* analysis above), we find that the HRI and IPC count rates of a pure hydrogen atmosphere are, respectively, 1.47 and 2.25 s^{-1}. By comparison, the reported observed count rates for Sirius B are 1.74 and 0.83 s^{-1} for the HRI and IPC, respectively. Hence, the actual HRI count rate agrees well ($\sim$17%) with the prediction based on a pure hydrogen atmosphere, whereas the observed IPC count rate is *smaller* than the predicted value by a factor $\sim$2.7. Taken at face value, this latter result would suggest that there is an extra opacity source in the atmosphere of Sirius B which depresses the flux in the IPC bandpass. The problem with this interpretation is that the observed HRI count rate should *also* have been significantly affected by this hypothetical opacity source, and it is not.

The situation is even more confused for HZ 43 because the atmospheric parameters for this object are still not well established. Indeed Heise et al. (1988) have not been able to fit satisfactorily a single model to the entire optical, UV, EUV, and X-ray spectral ranges. As an illustrative example, if we use a pure hydrogen atmosphere with $T_{\rm eff} = 52{,}000$ K, $\log g = 8.0$, and $\log n_{\rm H} = 18.9$, we find that the predicted count rates are 6.30 and 12.5 s^{-1} for the HRI and IPC detectors, respectively. The observed HRI and IPC count rates for HZ 43 are, respectively, 2.88 and 5.49 s^{-1}, roughly a factor of 2 smaller than the predicted values in both bandpasses. However, given the current unsatisfactory overall modeling of HZ 43, we have to give little weight to these differences in our comparison of the *Einstein* and *EXOSAT* observations.

To summarize, it appears that the *Einstein* IPC measurements are not consistent with the *EXOSAT* observations. This casts some doubts on the reality of the measured hydrogen layer masses in Table 4. In contrast, in the only two reliable cases for which we have both HRI and *EXOSAT* data (GD 246 and Sirius B), there exists a satisfactory consistency. In view of this, it may be difficult to explain the IPC discrepancies in terms of an unmodeled photospheric effect as mentioned above because the HRI flux would presumably also suffer from this effect. We cannot be completely certain at this stage, but it would appear that the IPC white dwarf measurements may suffer from some calibration uncertainties.

To complete our survey of the *EXOSAT* and *Einstein* observations of hot DA white dwarfs, we briefly consider the other targets which have been looked at but which we have not discussed previously. First, there is the question of the unsuspected presence of sdB stars in the target lists such as Feige 31 above. And indeed, the population of cataloged hot DA white dwarfs is contaminated to a certain extent by hot hydrogen-rich subdwarfs. It is usually difficult to separate the two populations based on low signal-to-noise optical spectra. There are a few examples of this in the sample of HRI observations selected by Petre et al. (1986) and in the *EXOSAT* observations presented by Paerels & Heise (1989). An inspection of the *IUE* low dispersion spectra for Feige 91 (SWP 25670 S and L) and EG 113 (SWP 22364 L) prescribes a rather low gravity for these objects based on the absence of the red wing of Lyα. The sdB classification of these objects precludes any detections in the EUV/soft X-ray range at the prescribed temperatures. Uncertainties on effective temperatures have also played a role. The 4 σ detection of GD 125 by Petre et al. may well be a statistical fluctuation in view of the new temperature we derived from an *IUE* low-dispersion image ($T_{\rm eff} = 23{,}700$ K; SWP 36031 L), and the nondetection of EG 226 with the HRI is no longer problematic since the actual temperature of this object is 21,700 K (SWP 33196 L) rather than 50,000 K.

4.3. *Stratified Atmospheres and the UV/Optical Properties of the DAB and DAO White Dwarfs*

The ultraviolet and optical spectroscopy of the prototypic DAB white dwarf GD 323 and of the DAO PG 1210+533 suggest the presence of helium distributed in a stratified hydrogen/helium configuration. Radiative levitation of helium has not the potential to bring into the photosphere the large abundance observed and accretion should leave traces of other elements that are not detected (see discussions in Vennes et al. 1988 and VTS). There is some evidence of a thin layer of hydrogen in GD 323: Liebert et al. (1984) have failed to reproduce the optical/UV energy distribution with any combination of H/He homogeneous atmospheres in a single star or even in a binary system while Koester (1989a) has suggested a possible fit using a H/He stratified atmosphere. This may not be the full story, however, because Figure 3 of Koester (1989a) suggests some problems in the fit to the observed *IUE* energy distribution. Short of a more detailed investigation (which is beyond the scope of the present paper), we can compare the observed equivalent width of the He I λ4471 feature in GD 323 (see Liebert et al. 1984) with our theoretical values in Table 1A. On this basis, we find a possible hydrogen layer mass $\log q_{\rm H} \sim -17$, in agreement with Koester (1989a).

The possibility of H/He stratification in G104−27 is based on the detection by Holberg et al (1990) of a weak He I λ4471 line with an equivalent width of 330 mÅ while He I λ4713 is distinctively absent from their spectrum. Using a model at $T_{\rm eff} = 25{,}000$ K (Table 1A) this would correspond to a hydrogen layer thickness of $\log q_{\rm H} = -16.2$. For such a thin layer, the helium convection zone (see Fig. 2) is located *below* the H/He transition zone and it is not clear whether it may disturb the diffusive equilibrium. In any case, the recent discussion presented by Kidder et al. (1992) clearly suggests that the presence of helium in the photospheric layers is time-dependent, so

a stratified model in strict diffusive equilibrium is probably not appropriate.

By contrast, the DAO white dwarfs offer promising insights in the study of stratification in hot H-rich white dwarfs and their progenitors. It has not been demonstrated yet that the very specific helium line shapes predicted by a stratified hydrogen/helium model can explain the observations. This will be a good test for stratified atmosphere hypothesis. The fact that helium is not homogeneously distributed tends to produce lines with very developed wings and no core to match them. Our preliminary study of PG 1210+533 indicates that the three lines, He I λ4471, He II λ1640, and He II λ4686 result in three slightly different hydrogen layer thicknesses of log q_H = -16.2, -16.0, and -16.4, respectively (Table 1B). This later value is extrapolated from Table 1B. The DAO PG 1305−017 presented by Holberg et al. (1989) seems to be a quite similar object. Holberg et al. have presented four hot DAO white dwarfs that constitute a sample of objects to study in parallel with the hot DA white dwarfs in which we find indirect evidence for a thin hydrogen layer.

5. DISCUSSION

We have presented a grid of H/He stratified model atmospheres for hot DA white dwarfs and have discussed some of their most important physical properties. In particular, synthetic spectra covering the soft X-ray to the FUV domains as well as the optical domain have been presented for representative cases. Our main motivation was to follow up on the original suggestion of Vennes et al. (1988) that the EUV/soft X-ray flux deficiency observed in many hot DA stars could be explained in terms of such models.

We have reanalyzed critically both the samples of objects observed with *EXOSAT* and *Einstein* in the context of our stratified models. To this end, we have provided, when possible, improved values of the atmospheric parameters in the cases where only rough estimates were available previously. In this effort, we have used archived *IUE* data and published optical photometry (see Vennes et al. 1990 for details on the method). Our analysis summarized in Table 5 shows that, out of 22 hot DA white dwarfs observed with *EXOSAT*, a total of eight do not show a EUV/soft X-ray flux deficiency and can be understood solely in terms of pure hydrogen atmospheres. We cannot decide yet on the reality of an extra opacity source in the atmosphere of six other objects either because the effective temperature is not known accurately enough or because the available short-wavelength data are insufficient (only one bandpass available or upper limits on count rates). The remaining eight objects definitely show a EUV/soft X-ray flux deficiency, however. Of those, the most interesting ones (from the point of view of this paper) are GD 2, GD 153, GD 394, and GD 246, which may show the presence of the helium diffusive tail in the photosphere. In contrast, the *EXOSAT* photometry of Feige 24 and G191 B2B cannot be understood in terms of H/He stratified atmospheres. Given the success of Vennes et al. (1989a) at explaining the EUV spectrum of Feige 24 in terms of a complex of heavy elements supported by radiative levitation, and given that G191 B2B has EUV photometric properties very similar to those of Feige 24, it is very likely that absorption by heavy elements is responsible for the EUV/soft X-ray flux deficiency in G191 B2B as well. The stratified atmosphere hypothesis may yet apply for the peculiar DA white dwarf V471 Tau since a fit to the photometric data is obtained for a hydrogen layer mass log $q_H = -13.45$. However, because of the possibility of accretion from its companion and the formation of X-ray opaque poles (Jensen et al. 1986, but see also Clemens et al. 1992), we do not include V471 Tau in the list of most likely candidates for atmospheric stratification. Finally, the EUV/soft X-ray opacity of G104−27 is more likely related to transient appearance of helium in its atmosphere possibly caused by mixing event (Kidder et al. 1992), and the stratified atmosphere model probably does not apply in this case.

Our analysis of six objects observed with *Einstein* suggests that, in all cases, there is a EUV/soft X-ray flux deficiency and, therefore, we have formally obtained a value of the atmospheric hydrogen layer mass that could explain this deficiency (Table 4). However, we have found inconsistencies between the *EXOSAT* photometry and the *Einstein* IPC count rates for stars in common in the two samples. In contrast, the *Einstein* HRI data appear quite consistent with the *EXOSAT* data for two objects (Sirius B ad GD 246) which have been observed in common. We believe that there could be some residual calibration errors in the IPC at very low energies. In view of this, we suggest that the *Einstein* IPC observations of hot DA white dwarfs should be considered with caution.

We note that HZ 43 (assigned to our group of pure hydrogen atmosphere objects) has still not been modeled satisfactorily despite the potential high quality of its *EXOSAT* spectroscopic and photometric data sets (Heise et al. 1988; Paerels et al. 1986a). The purity of its atmosphere cannot be questioned because neither *IUE* high-dispersion spectra (VTS) nor the *EXOSAT* spectra have revealed the presence of trace elements down to very significant limits. Likewise, errors in the computed fluxes must be ruled out because, in a pure hydrogen

TABLE 5

RESULTS ON THE TYPES OF ATMOSPHERES SUGGESTED BY THE *EXOSAT* DATA SET

	PURE HYDROGEN OR POTENTIALLY STRATIFIED				
Pure Hydrogen	Critical T_{eff} Range	Insufficient Data	Potentially Stratified	Not Stratified	Others
GD 257	GD 659[a]	WD 0416−551	GD 2[a]	Feige 24[a]	V471 Tau
GD 71[a]	LB 1663[a]	VR 16	GD 153[a]	G191 B2B[a]	G104−27[a]
Sirius B[a]	WD 2000−562	Feige 106	GD 394[a]		
LTT 3870[a]			GD 246[a]		
CoD−38°10980[a]					
PG 1658+441					
GD 391[a]					
HZ 43[a]					

[a] From VTS.

context, stellar atmosphere theory provide, at the effective temperature characteristic of HZ 43 ($T_{\rm eff} \approx 52{,}000$ K), very accurate fluxes ($\Delta H_\nu < 1\%$) for the entire spectral range of interest. We tentatively suggest that our failure to provide a unique solution to HZ 43 within the 1 σ error bars of all filtered photometry of *EXOSAT* must be related to fine-tuning uncertainties in the instrumental calibration. Nevertheless, we support the basic conclusion of Heise et al. (1988) that HZ 43 has a lower effective temperature, $T_{\rm eff} \approx 52{,}000$ K, than previously thought.

A comment must be made about the number (4) of stars which we have retained from our *EXOSAT* analysis as most likely to have a stratified atmosphere. This number is significantly less than that presented in the preliminary study of Vennes et al. (1989b) which is based on a subset of the sample of stars used here (see also Koester 1989a, b). Vennes et al. (1989b) considered a subset of 14 stars observed with *EXOSAT* and assigned preliminary values of log $q_{\rm H}$ to eight stars including GD 659, LB 1663, G191 B2B, GD 257, and GD 391, which we have not retained in the present study. The three other objects (GD 153, GD 394, and GD 246) remain likely candidates for atmospheric stratification. As indicated above, our more detailed analysis now allows us to rule out the stratified atmosphere hypothesis for G191 B2B. As for GD 257 and GD 391, our downward revisions and improved estimates of their effective temperatures indicate that their spectral properties are now entirely consistent with pure hydrogen models. To account for the observed EUV/soft X-ray count rates, the larger earlier values of the effective temperature did require an additional opacity source. For LB 1663, our downward revision of its effective temperature places that star in a critical range of temperatures where no firm conclusion can be reached yet as to presence of an additional opacity source. A very accurate determination of its effective temperature is required for deciding on the issue, and provisionally, we have not retained LB 1663 as a candidate for atmospheric stratification. Our more stringent criteria used here also explain why we have not retained GD 659 either, another example of an object whose effective temperature is in a critical range for determining the reality of a EUV/soft X-ray flux deficiency.

Similar remarks can be made about the analysis reported in Vennes et al. (1988). These authors estimated hydrogen layer masses in 10 hot DA objects (see their Fig. 8) for which a EUV/soft X-ray flux deficiency had been reported previously either from *EXOSAT* or *Einstein* observations. For reasons discussed above, we remove five stars from that list: GD 659, Feige 24, LB 1663, G191 B2B, and GD 257. In addition, we also remove GD 50 and GD 125 because these stars have been observed only with the *Einstein* IPC detector and, as mentioned above, there could be some residual calibration problems with this detector for extremely soft sources. Hence, in the light of the present results, only three objects (GD 153, GD 394, and GD 246) remain from the list considered originally by Vennes et al. (1988) as genuine candidates for atmospheric stratification. We note also that the *upward* revision of the effective temperature of GD 2 proposed by Vennes et al. (1990) makes that star another candidate. On the basis of the preliminary effective temperature suggested by Petre & Shipman (1987), Vennes et al. (1988) had considered GD 2 as a pure hydrogen atmosphere star.

The rather stringent and conservative criteria which we have used here leave us with a short list of four stars (GD 2, GD 153, GD 246, and GD 394) which, potentially, have stratified atmospheres. In this connection, it is of interest to recall that Vennes et al. (1988) have demonstrated that, at a given wavelength, there is a one-to-one correspondence between the helium abundance inferred on the basis of an uniformly mixed H/He atmosphere and the hydrogen layer mass in a stratified model. In principle, this correspondence does not generally hold when several bandpasses are simultaneously used, but Vennes et al. (1988) have nevertheless called to the attention the fact that layered H/He atmospheres cannot be easily distinguished from uniformly mixed H/He atmospheres on the basis of *EXOSAT* broad-band photometry alone. This is a point which has also been made by Koester (1989a, b). Part of the problem here is that only a minority of DA stars have been detected in more than two bandpasses by *EXOSAT* (eight objects out of 21). Even for these objects, however, the spectral resolution offered by *EXOSAT* broad-band photometry remains somewhat inadequate. We nevertheless note that the careful study of GD 2 carried out by Vennes et al. (1990) does suggest that the formal fit of *EXOSAT* broad-band colors to theoretical fluxes is marginally better for stratified than uniform atmospheres. This may indicate that the former are more appropriate in the analysis of such broad-band photometry. Of course, EUV *spectroscopy* would indicate clearly which of the two types of models best accounts for the observations as their spectral signatures become quite distinct at high enough resolution (see Vennes et al. 1989b). We strongly suspect, however, that such comparison may be more of academic interest than of practical value because homogeneously mixed H/He models of hot DA white dwarfs are not expected to exist in Nature (Vennes et al. 1988).

On the other hand, we cannot dismiss yet the possibility that absorption by heavy elements plays a role (perhaps even the dominant one) on the spectral properties of the four stars we have retained. After all, theoretical considerations indicate that a host of heavy elements may levitate under the influence of selective radiative forces in the atmospheres of hot white dwarfs (Vauclair, Vauclair, & Greenstein 1979; Morvan, Vauclair, & Vauclair 1986; Chayer et al. 1987; Chayer, Fontaine, & Wesemael 1989, 1991). The picture is somewhat complicated by the fact that weak stellar winds may play havoc with the expected heavy element abundances in the photospheric layers (Chayer et al. 1987, 1989). Nevertheless, it is in this theoretical framework that Vennes et al. (1989a) have presented a convincing explanation for the EUV spectrum of Feige 24. This success underlined the fact that Vennes et al. (1988) may have been somewhat optimistic as to the role of atmospheric stratification as a *general* explanation for the EUV/soft X-ray flux deficiency observed in many hot DA white dwarfs. For instance, as in the case of Feige 24, it is now very likely that absorption by heavy elements also controls the EUV/soft X-ray flux of G191 B2B. However, it has been argued that absorption by heavy elements may not hold the full story either for the four candidates we have retained as well as for other stars (VTS). The survey of high-resolution spectra of all hot DA white dwarfs observed with *IUE* carried out by VTS has failed to reveal the presence of C, N, and Si in the photospheres of our four candidates. Another circumstantial evidence is that solutions consistent with the idea of layered atmospheres have been obtained for these candidates in our analysis of *EXOSAT* data, while this idea had to be rejected for both Feige 24 and G191 B2B. This suggest that *EXOSAT* broad-band photometry allows some discrimination between the two types of model atmospheres, at least when the abun-

dances of heavy elements are at the level as those found in Feige 24 (and presumably in G191 B2B). However, when the observed departure from a pure hydrogen atmosphere is a small perturbation (e.g., GD 153) this constitutes only a weak evidence. We have indicated in Table 5 which stars have been examined by VTS. Only upper limits on photospheric abundances of C, N, and Si have been obtained for all the stars indicated in the first four columns of the table. In contrast, photospheric traces of C, N, and Si have been detected in the *IUE* spectra of both Feige 24 and G191 B2B. More recently, traces of Fe were also discovered and abundances estimated in the photosphere of these two stars (Vennes et al. 1992). The failure to detect heavy elements in the spectra of our four candidates (as well as other DA stars) suggests that these atmospheres may be free of heavy elements and that atmospheric stratification may be necessary in those cases. This failure does not constitute a firm proof by itself, however, because one can easily imagine that traces of C, N, and Si smaller than the derived upper limits in the VTS survey could combine to many other elements, not visible in the *IUE* window, but present in small abundances, such that their collective effects may have an appreciable impact on the EUV flux. Fortunately, as shown by Vennes et al. (1989a), absorption by heavy elements leaves a characteristic spectral signature in the EUV domain which is quite distinct from that of layered H/He atmospheres. Hence, *EUV spectroscopy will be necessary to discriminate between absorption by heavy elements and atmospheric H/He stratification.* The advent of the *EUVE* should provide us with the definitive answer as to the relative importance of these two configurations in hot DA white dwarfs. This may prove to be the most significant contribution of *EUVE* to the white dwarf field.

Pending the results of such observations, it is interesting to reconsider the relationship between the effective temperature and the EUV/soft X-ray flux deficiency (caused by either atmospheric stratification or absorption by heavy elements or both) observed in hot DA white dwarfs. For our purposes, we retain only the stringent selection criteria which we used in our own analysis of the *EXOSAT* sample, and we specifically exclude the peculiar objects V471 Tau and G104−27. We first find (see Tables 2 and 5) that six objects out of six with effective temperatures less than $T_{\rm eff} \approx 35{,}000$ K all have pure hydrogen atmospheres (to the sensitivity limits of present-day detectors). In contrast, we also find that six objects out of eight hotter than this value do show a EUV/soft X-ray flux deficiency, the two exceptions being GD 257 and HZ 43. We believe it is significant that three stars for which we cannot decide yet on the reality of a EUV/soft X-ray flux deficiency all have effective temperatures near 35,000 K: GD 659 ($T_{\rm eff} \approx 37{,}000$ K), LB 1663 ($T_{\rm eff} \approx 32{,}000$ K), and WD 2000−562 ($T_{\rm eff} \approx 36{,}000$ K). The uncertainties on effective temperatures of these stars are no worse systematically than cooler or hotter star in the sample, but the objects clearly sit in a critical range of effective temperature where much improved values of $T_{\rm eff}$ will be needed to decide whether or not they have pure hydrogen atmospheres or atmospheres polluted by some trace absorbers. It thus seems that a majority of hot DA white dwarfs have some pollutants in their atmospheres for $T_{\rm eff} \geq 35{,}000$ K, but that the phenomenon disappears below this temperature. Clearly, any model proposed to account for the spectral properties of hot DA white dwarfs must be consistent with this phenomenon.

Qualitatively speaking, both atmospheric stratification and absorption by heavy elements can be made compatible with this observation. In the latter case, we know that selective radiative support diminishes with decreasing effective temperature, and that weak stellar winds could empty the reservoirs of levitating heavy elements on relatively short time scales (cf. Chayer et al. 1987, 1989). The details are being worked out, however. In the case of atmospheric stratification, Vennes et al. (1988) have pointed out that cooling pushes the photosphere higher up at smaller mass fraction and, consequently the possibility of detecting the helium diffusive tail decreases for cooler objects. Moreover, Fontaine & Wesemael (1987) have suggested that DA white dwarf atmospheres could be formed by the migration of hydrogen from deep regions of the envelope where it is initially mixed to the surface where it accumulates. Depending on the initial total mass of hydrogen and its distribution, the separation process may last up to a few million years (the details are again being worked out). In this scenario, the hot phase of DA evolution is characterized by the continuous buildup of the outer hydrogen layer until the separation process has been completed. Hence, as evolution proceeds, the thickness of the hydrogen outer layer increases until the helium diffusive tail becomes totally buried, out of reach of the EUV detectors which may probe the outermost layers. With only four objects in our current sample of DA stars for which $q_{\rm H}$ has been inferred, it is difficult to observe a trend (if any) between hydrogen layer mass and effective temperature. However, considering the lower limits we have inferred on $q_{\rm H}$ for the (cooler) pure hydrogen stars, and the approximate value of $\log q_{\rm H} \approx -15$ in DAO stars (taking into account the dilution of hydrogen in the helium convection zone as pointed out by MacDonald & Vennes 1991), there seems to be a trend in the sense expected, i.e., lower temperature stars tend to have larger hydrogen layer masses. Note that this trend certainly need to be confirmed by additional observations.

Finally, we note this apparent trend between inferred hydrogen layer mass and effective temperature in hot DA white dwarfs, first discussed by Vennes et al. (1988), who used a simple formalism for estimating $q_{\rm H}$. We find that this formalism is accurate enough, reproducing (within a factor of 2) the values of $q_{\rm H}$ obtained here on the basis of our detailed model atmosphere calculations. Contrary to an assertion found in Koester (1989a, b) and Koester et al. (1990), the Vennes et al. (1988) formalism *does* take into account the nonhomogeneous distribution of helium in layered atmospheres. The main difference between the results of Vennes et al. (1988) and the present analysis comes from their choice of one representative wavelength for both *EXOSAT* and *Einstein* (85 Å) instead of using the integrated bandpasses of the instrumental configurations.

S. V. would like to thank Harry Shipman for his support while this paper was in preparation. We are also indebted to Jim MacDonald for several comments on the manuscript and Frits Paerels for sharing with us his knowledge of the *EXOSAT* calibration. We acknowledge partial support from NASA (NAG 5-972), NSF (AST 87-20530), NSERC Canada, and the Fund FCAR (Québec). G. F. also enjoyed the support of a Killam Fellowship.

REFERENCES

Arcoragi, J.-P., & Fontaine, G. 1980, ApJ, 242, 1208
Auer, L. H., & Mihalas, D. 1972, ApJS, 24, 193
Auer, L. H., & Shipman, H. L. 1977, ApJ, 211, L103
Bergeron, P., Kidder, K. M., Holberg, J. B., Liebert, J., Wesemael, F., & Saffer, R. A. 1991, ApJ, 372, 267
Bois, B., Lanning, H. H., & Mochnacki, S. W. 1988, AJ, 96, 157
Bruhweiler, F. C., & Kondo, Y. 1983, 269, 657
Chayer, P., Fontaine, G., & Wesemael, F. 1989, in IAU Colloq. 114, White Dwarfs, ed. G. Wegner (Berlin: Springer), 253
———. 1991, in White Dwarfs, ed. G. Vauclair & E. Sion (Dordrecht: Kluwer), 249
Chayer, P., Fontaine, G., Wesemael, F., & Michaud, G. 1987, in IAU Colloq. 95, The Second Conference on Faint Blue Stars, ed. A. G. D. Philip, D. S. Hayes, & J. Liebert (Schenectady: Davis), 653
Clemens, J. C., et al. 1992, ApJ, 391, 773
Dimitrijevic, M. S., & Sahal-Bréchot, S. 1984a, A&A, 136, 289
———. 1984b, J. Quant. Spectros. Rad. Transf., 31, 301
Dupree, A. K., & Raymond, J. C. 1982, ApJ, 263, L63
Dziembowski, W., & Koester, D. 1981, A&A, 97, 16
Finley, D. S., Basri, G., & Bowyer, S. 1990, ApJ, 359, 483
Fontaine, G., & Wesemael, F. 1987, in IAU Colloq. 95, The Second Conference on Faint Blue Stars, ed. A. G. D. Philip, D. S. Hayes, & J. Liebert (Schenectady: Davis), 319
Green, J., Jelinsky, P., & Bowyer, S. 1990, ApJ, 359, 499
Guinan, E. F., & Sion, E. M. 1984, AJ, 89, 1252
Hearn, A. G., & Mewe, R. 1976, A&A, 50, 319
Heise, J., & Huizenga, H. 1980, A&A, 84, 280
Heise, J., Paerels, F. B. S., Bleeker, J. A. M., & Brinkman, A. C. 1988, ApJ, 334, 958
Holberg, J. B. 1984, in IAU Colloq. 81, Local Interstellar Medium, ed. Y. Kondo, F. C. Bruhweiler, & B. D. Savage (NASA CP-2345), 91
Holberg, J. B., Kidder, K., Liebert, J., & Wesemael, F. 1989, in IAU Colloq. 114, White Dwarfs, ed. G. Wegner (Berlin: Springer), 188
Holberg, J. B., Kidder, K. M., & Wesemael, F. 1990, ApJ, 365, L77
Holberg, J. B., Sandel, B. R., Forrester, W. T., Broadfoot, A. L., Shipman, H. L., & Barry, D. C. 1980, ApJ, 242, L119
Holberg, J. B., Wesemael, F., & Basile, J. 1986, ApJ, 306, 629
Holberg, J. B., Wesemael, F., & Hubeny, I. 1984, ApJ, 280, 679
Holberg, J. B., Wesemael, F., Wegner, G., & Bruhweiler, F. C. 1985, ApJ, 293, 294
Jelinsky, P. N. 1988, Ph.D. thesis, Univ. California, Berkeley
Jensen, K. A., Swank, J. H., Petre, R., Guinan, E. F., Sion, E. M., & Shipman, H. L. 1986, ApJ, 309, L27
Jordan, S., & Koester, D. 1986, A&AS, 65, 367
Jordan, S., Koester, D., Wulf-Mathies, C., & Brunner, H. 1987, A&A, 185, 253
Kahn, S. M., Wesemael, F., Liebert, J., Raymond, J. C., Steiner, J. E., & Shipman, H. L. 1984, ApJ, 278, 255
Kidder, K. M., Holberg, J. B., Barstow, M. A., Tweedy, R. W., & Wesemael, F. 1992, preprint
Kidder, K. M., Holberg, J. B., & Mason, P. A. 1991, AJ, 101, 579
Kidder, K., Holberg, J. B., & Wesemael, F. 1989, in, IAU Colloq. 114, White Dwarfs, ed. G. Wegner (Berlin: Springer), 350
Koester, D. 1989a, in IAU Colloq. 114, White Dwarfs, ed. G. Wegner (Berlin: Springer), 206
———. 1989b, ApJ, 342, 999
Koester, D., Beuermann, K., Thomas, H.-C., Graser, U., Giommi, P., & Tagliaferri, G. 1990, A&A, 239, 260
Liebert, J., Schmidt, G. D., Green, R. F., Stockman, H. S., & McGraw, J. T. 1983, ApJ, 264, 262
Liebert, J., Wesemael, F., Sion, E. M., & Wegner, G. 1984, ApJ, 277, 694
MacDonald, J., & Vennes, S. 1991, ApJ, 371, 719
Malina, R. F., Bowyer, S., & Basri, G. 1982, ApJ, 262, 717
Margon, B., Bolte, M., & Anderson, S. F. 1987, AJ, 93, 1229
Margon, B., Lampton, M., Bowyer, S., Stern, R., & Paresce, F. 1976, ApJ, 210, L79
McCook, G. P., & Sion, E. M. 1987, ApJS, 65, 603
Mihalas, D. 1978, Stellar Atmospheres (San Francisco: Freeman)
Mihalas, D., Auer, L. H., & Heasley, J. N. 1975, NCAR Tech. Note STR-104
Morvan, E., Vauclair, G., & Vauclair, S. 1986, A&A, 163, 145
Muchmore, D. 1982, ApJ, 259, 749
Mullan, D. J., Shipman, H. L., Sion, E. M., & MacDonald, J. 1991, ApJ, 374, 707
Paerels, F. B. S., Bleeker, J. A. M., Brinkman, A. C., Gronenschild, E. H. B. M., & Heise, J. 1986a, ApJ, 308, 190
Paerels, F. B. S., Bleeker, J. A. M., Brinkman, A. C., & Heise, J. 1986b, ApJ, 309, L33
———. 1988, ApJ, 329, 849
Paerels, F. B. S., Brinkman, A. C., Boggende, A. J. F., de Korte, P. A. J., & Dijkstra, J. 1990, A&AS, 85, 1021
Paerels, F. B. S., & Heise, J. 1989, ApJ, 339, 1000
Pelletier, C., Fontaine, G., Wesemael, F., Michaud, G., & Wegner, G. 1986, ApJ, 307, 242
Petre, R., & Shipman, H. L. 1987, BAAS, 19, 1041
Petre, R., Shipman, H. L., & Canizares, C. R. 1986, ApJ, 304, 356
Pravdo, S. H., Marshall, F. E., White, N. E., & Giommi, P. 1986, ApJ, 300, 819
Reid, N., & Wegner, G. 1988, ApJ, 335, 953
Schöning, T., & Butler, K. 1989a, A&AS, 78, 51
———. 1989b, A&AS, 79, 153
Shipman, H. L. 1976, ApJ, 206, L67
Shipman, H. L., Margon, B., Bowyer, S., Lampton, M., Paresce, F., & Stern, R. 1977, ApJ, 213, L25
Stanghellini, L., Starrfield, S., & Cox, A. N. 1990, A&A, 233, L13
Thejll, P., Shipman, H. L., MacDonald, J., & MacFarland, W. M. 1990, ApJ, 361, 197
Unglaub, K., & Bues, I. 1991, in White Dwarfs, ed. G. Vauclair & E. Sion (Dordrecht: Kluwer), 267
Vaiana, G. S., et al. 1981, ApJ, 244, 163
Vauclair, G., Vauclair, S., & Greenstein, J. L. 1979, A&A, 80, 79
Vennes, S. 1988, Ph.D. thesis, Univ. Montréal
———. 1990, ApJ, 361, L65
Vennes, S., Chayer, P., Fontaine, G., & Wesemael, F. 1989a, ApJ, 336, L25
Vennes, S., Chayer, P., Thorstensen, J. R., Bowyer, S., & Shipman, H. L. 1992, ApJ, 392, L27
Vennes, S., Fontaine, G., & Wesemael, F. 1989b, in IAU Colloq. 114, White Dwarfs, ed. G. Wegner (Berlin: Springer), 368
Vennes, S., Pelletier, C., Fontaine, G., & Wesemael, F. 1988, ApJ, 331, 876
Vennes, S., Shipman, H. L., & Petre, R. 1990, ApJ, 364, 647
Vennes, S., Thejll, P., & Shipman, H. L. 1991a, in White Dwarfs, ed. G. Vauclair & E. Sion (Dordrecht: Kluwer), 235 (VTS)
Vennes, S., Thorstensen, J. R., Thejll, P., & Shipman, H. L. 1991b, ApJ, 372, L37
Vidal, C. R., Cooper, J., & Smith, E. W. 1973, ApJS, 25, 37
Werner, K., Heber, U., & Hunger, K. 1991, A&A, 244, 437
Wesemael, F., Green, R. F., & Liebert, J. 1985, ApJS, 58, 379.